Deterministic Lateral Displacement for Cell Separation

Tran, Si Hoai Trung

2019

Document Version:
Publisher's PDF, also known as Version of record

Deterministic Lateral Displacement for Cell Separation

TRUNG SI HOAI TRAN
FACULTY OF ENGINEERING | LUND UNIVERSITY

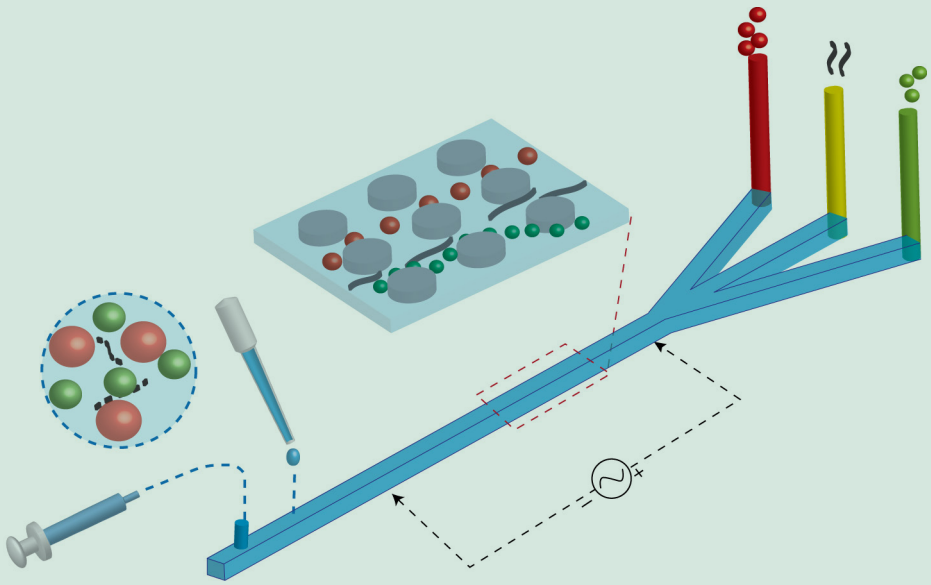

Deterministic Lateral Displacement for Cell Separation

Trung Si Hoai Tran

LUND
UNIVERSITY

DOCTORAL DISSERTATION

by due permission of the Faculty of Engineering, Lund University, Sweden.
To be defended at Rydbergssalen, Sölvegatan 14. Date June 14th, and time 09:15.

Faculty opponent:

Professor Nikolaj Gadegaard

University of Glasgow

Organization	Document name
LUND UNIVERSITY	**DOCTORAL DISSERTATION**
Department of Physics Professorsgatan 1 223 63 Lund, Sweden	Date of disputation **2019-06-14**
	Sponsoring organization
Author(s) **Trung Si Hoai Tran**	

Title and subtitle

Deterministic Lateral Displacement for Cell Separation

Abstract

In the fields of medicine and biology, the separation of particles is a central step in many preparative and analytical processes. *Deterministic Lateral Displacement (DLD)* has been a promising technique in the field of microfluidic particle and cell sorting, specifically for label-free separation with several applications of sorting by size, morphology, and deformation reported in the literature over the last decade.

Separation of cancer cells from a heterogeneous sample is known as a challenging task due to the similarity of the cells involved. Deformability is a potential bio-marker for cell isolation where specific molecular markers are lacking. In the thesis, we demonstrate an efficient measurement tool for cell deformation in the DLD device as well as a sorting tool for cell isolation based on deformability among breast cancer cells (MCF7), human breast cells (MCF10A) and metastasizing breast cancer cells (MDA-MB-231). (Paper 2).

Many sorting problems require careful optimization for a successful result. We have approached this problem in two ways: a combination of electrokinetics and DLD for controlling the rotation of RBCs (Paper 3) or through the deformation of the DLD devices by control of the driving pressure (Paper 5).

An important limitation of microfluidics is that conventional pumps are difficult to transport, need trained personnel and are associated with high running costs. They are often not fully compatible with point-of-care applications, especially in resource-poor settings. The second part of this thesis therefore focuses on alternative ways to operate microfluidic DLD devices, to ensure portability and user friendliness. A combination of an open DLD device and a paper-based pump is a key component of this approach (Paper 1). Several sorting applications involving blood fractionation, trypanosome enrichment, and breast cancer cell extraction are performed efficiently in terms of potential purity and capture rate. Moreover, our open-fluidics platform is shown to have advantages with regards to easy cleaning, reusability and electrokinetic integration. Finally, an approach for fast and easy fabrication for devices based on single or multilayer stacks is discussed in Paper 4.

Key words

Label-free separation, Deterministic Lateral Displacement, Deformability-based sorting

Classification system and/or index terms (if any)

Supplementary bibliographical information		Language **English**
ISSN and key title		**ISBN** 978-91-7895-139-0 (print) 978-91-7895-140-6 (pdf)
Recipient's notes	**Number of pages** 125	Price
	Security classification	

Signature  Date 2019-05-09

Deterministic Lateral Displacement for Cell Separation

Trung Si Hoai Tran

LUND
UNIVERSITY

Cover illustration front and back by Trung Si Hoai Tran.

Faculty of Engineering,
Department of Physics

978-91-7895-139-0 (print)
978-91-7895-140-6 (pdf)

Printed in Sweden by Media-Tryck, Lund University
Lund 2019

To my parents and family

Table of Contents

Abstract

In the fields of medicine and biology, the separation of particles is a central step in many preparative and analytical processes. *Deterministic Lateral Displacement (DLD)* has been a promising technique in the field of microfluidic particle and cell sorting, specifically for label-free separation with several applications of sorting by size, morphology, and deformation reported in the literature over the last decade.

Separation of cancer cells from a heterogeneous sample is known as a challenging task due to the similarity of the cells involved. Deformability is a potential biomarker for cell isolation where specific molecular markers are lacking. In the thesis, we demonstrate an efficient measurement tool for cell deformation in the DLD device as well as a sorting tool for cell isolation based on deformability among breast cancer cells (MCF7), human breast cells (MCF10A) and metastasizing breast cancer cells (MDA-MB-231) (Paper 2).

Many sorting problems require careful optimization for a successful result. We have approached this problem in two ways: a combination of electrokinetics and DLD for controlling the rotation of RBCs (Paper 3) or through the deformation of the DLD devices by control of the driving pressure (Paper 5).

An important limitation of microfluidics is that conventional pumps are difficult to transport, need trained personnel and are associated with high running costs. They are often not fully compatible with point-of-care applications, especially in resource-poor settings. The second part of this thesis therefore focuses on alternative ways to operate microfluidic DLD devices, to ensure portability and user friendliness. A combination of an open DLD device and a paper-based pump is a key component of this approach (Paper 1). Several sorting applications involving blood fractionation, trypanosome enrichment, and breast cancer cell extraction are performed efficiently in terms of potential purity and capture rate. Moreover, our open-fluidics platform is shown to have advantages with regards to easy cleaning, reusability and electrokinetic integration. Finally, an approach for fast and easy fabrication for devices based on single or multilayer stacks is discussed in Paper 4.

Popular Summary in English

Cancer is the second leading cause of death globally (only after heart disease according to the World Health Organization (WHO) 2018). Early diagnosis is the key to higher survival rates, reduced morbidity and treatment costs. Enormous research effort has been dedicated to create diagnosis tools with high efficiency, low cost, reduced time consumption and ease of operation.

Microfluidics, the handling of fluids in micro-scale environments, has great potential to address these challenges. The field has grown rapidly and demonstrated high impact on life science research and diagnosis techniques in the last two decades. In cancer, microfluidics shows promise for better diagnosis, and also serves as an emerging tool to study cancer biology. With the benefits of small sample volumes, multiplexing capabilities, quick operation, and highly sensitive analysis, microfluidics is valuable for cancer detection and investigation. Microfluidic systems have provided an advantageous environment for cancer cell studies such as cellular transduction, cell growth and division, and drug screening. In addition, to detect, isolate and enrich cancer cells, a variety of microfluidic sorting techniques have been successfully exploited.

In terms of biomedical particle separations and fractionations, microfluidic technologies, compared to traditional methods, provide the advantage of reducing operational complexity, small footprint and portability, and the possibility of multiplexing and integration. To contribute to the field of particle separation, the aim of this thesis is to propose a biomedical sorting tool with potential for high efficiency and high throughput that also has potentially low cost and high ease-of-use. By exploring different physical properties of the typical sample (normal and cancerous cells) including size, morphology, electrical/dielectric properties and deformation, this work makes advances towards high efficiency sorting for cancer cell analysis. Another aspect of this work is to simplify microfluidic separation devices. An optimization process is conducted through design automation, simplified fabrication and tunable operation. The study presented here is a modest attempt to contribute to the future of point-of-care diagnostics.

Acknowledgements

First of all, I would like to thank Prof. Jonas Tegenfeldt and Dr. Jason Beech for their support during my Ph.D. for over last four and a half years. Their knowledge and deep insight in physics, and specifically in microfluidics and Deterministic Lateral Displacement have been very valuable, and been a source of inspiration and encouragement. Thanks also to Dr. Stefan Holm for his help with microfabrication and support in the lab. My good group mates, Kush and Oskar, are also my good friends. Thanks for the nice chats and jokes. A big thank to Bao, a colleague, a friend, and a brother.

I am grateful to be a member of the biogroup: Christelle, Heiner, Jonas, Laura, Elke, Fei Fei, Mercy, Martin, Frida, Regina, Kalle, Therese, Roman, Jingyuan, Pradheebha, Ivan, who have given helpful comments about my works during our weekly meetings. I also feel thankful to the faculty, administrative, and technical staff at FTF, who have directly helped me during my PhD or have contributed to building a supportive working environment I enjoy every day: Dan, Jonas Johansson, Anneli, Anders Gustafsson, Maria, Johanna, Janne, Bengt, Håkan, Marica, Mia, Sara, Mariusz, Abdul-Rehman, Charlotte and Helena. And the list goes on. Thank you all for the time I have been at FTF.

I would also like to thank all my colleagues, for a lot of nice discussions and experienced comments that contributed to the scientific dialogue in this Ph.D dissertation, the entire Bio-group at the Division of Solid State Physics, Lund University. The vibrant atmosphere and interesting discussions in this group were a true pleasure to experience. Also, Prof. Bo Baldetorp and his colleagues have been a great help during my projects.

Last but not least, special thanks are due to my parents and family.

Con xin cám ơn ba Toán, má Lang, bố Hòa và mẹ Thọ và các anh chị trong gia đình mình đã luôn động viên, ủng hộ và giúp đỡ em trong suốt những năm qua. Xin cám ơn em, Thùy Dung, người đã luôn ở bên cạnh và đồng hành cùng anh trong bất cứ hoàn cảnh nào. Với tất cả yêu thương, papa xin dành tặng cho hai tình yêu nhỏ bé Thùy Nhi và Minh Duy.

List of Publications

The following research papers and manuscripts are included in this thesis:

I. **Open channel deterministic lateral displacement for particle and cell sorting** (published)

Trung S.H. Tran, Ho, Bao D., Beech, Jason P., Tegenfeldt, Jonas O.

Lab on a Chip, 2017. [DOI: 10.1039/C7LC00707H]

I performed the majority of the experimental work, and analyzed the data. B. Ho contributed to the experiments of electrical measurements. J.P. Beech performed confocal microscopy and macro photography. I wrote the manuscript together with J.P. Beech.

II. **Softness sorting of cancer cells in deterministic lateral displacement** (manuscript)

Trung S.H. Tran, Jason P. Beech and Jonas O. Tegenfeldt.

I performed all the experiments, analyzed the data and wrote the manuscript.

III. **Electrokinetic Rotation of Red Blood Cells in Deterministic Lateral Displacement devices** (manuscript)

Bao D. Ho*, Trung S.H. Tran*, Jason P. Beech and Jonas O. Tegenfeldt.

I contributed to conducting experiments, data analysis and wrote the manuscript together with Bao Ho. I did not contribute to investigate the electric/dielectric properties of the sample.

IV. Rapid duplication and alignment for multiplayers of microfluidic PDMS devices (manuscript)

Trung S.H. Tran, Bao D. Ho, Oskar E Ström, Jason P. Beech and Jonas O. Tegenfeldt.

I performed the experiments and analyzed the data. B. Ho verified and optimized the procedure. Oskar performed scanning electron microscopy. I wrote the manuscript together with B. Ho.

V. Tunable separation in deterministic lateral displacement by pressure control on varying PDMS stiffness (manuscript)

Trung S.H. Tran, Bao D. Ho, Jason P. Beech and Jonas O. Tegenfeldt.

I performed all the experiments, analyzed the data and wrote the manuscript. Bao Ho simulated the *in-silico* model.

List of Abbreviations

CAD	Computer-Aided Design
BSA	Bovine serum albumin
DI water	Deionized water
DLD	Deterministic Lateral Displacement
G	DLD gap distance
MCF7	Michigan Cancer Foundation-7 (breast cancer cell line)
MCF10A	Michigan Cancer Foundation-10A (human breast cell line)
MDA-MB-231	M.D. Anderson – Metastasis Breast Cancer-231 (Metastasis breast cell line)
LOC	Lab-On-a-Chip
PDMS	Poly-Di-Methyl-Siloxane
PLL-(g)-PEG	Poly (L-Lysine)-graft-Polyethylene glycol
POC	Point-of-care
RBCs	Red Blood Cells
R_C	Critical Radius
WBCs	White Blood Cells
GFP	Green Fluorescent Protein

Cancer Cell Analysis and Microfluidics: Cell Separation

Cancer is a class of pathologies characterized by uncontrolled growth and division of cells. With early detection, a proper treatment can be selected and thus assist in the curing process. Within *in-vitro* cancer cell diagnostics, microfluidics is a promising approach, and an alternative to traditional techniques, to provide efficient and rapid analysis. The current section discusses the role of microfluidics in cancer analysis, with specific focus on cell separation.

Microfluidic approaches for cancer analysis

Among the growing number of potential methods for cancer analysis, microfluidics is being rapidly developed to be a highly promising approach, and has been contributing to the knowledge of cancer. In the last two decades, it has addressed several fundamental scientific questions and biomedical challenges including the areas of diabetes, stroke and cytometry. In terms of cancer analysis, these micro-devices provides new promising tools for cancer detection, cell separation, cell/tissue culture, the study of cell mechanics, and integrated analysis systems (1).

In experimental cell biology, microchips for cell culture have become more and more common. In addition to the traditional cell culture systems (polystyrene dishes, flasks or well-plates), microchips offer an advantageous platform, which mimics the cellular environment, as well as provides flexible control for administration and extraction of reagents and fluids for cell analysis. Figure 1 summarizes several key differences between the macroscopic and microfluidic cell culture. The first advantage of microfluidic cell culture is the high flexibility of the designs to target specific cells in typical experiments. Small volumes, low reagent consumption and the ability to work with a small number of cells are among the unique strengths of microfluidic systems compared to macroscopic cultures. Furthermore, microfluidics

facilitates the realization of any necessary 3D environment, co-culturing as well as real-time on-chip analysis, which cannot be conducted in conventional culturing (2).

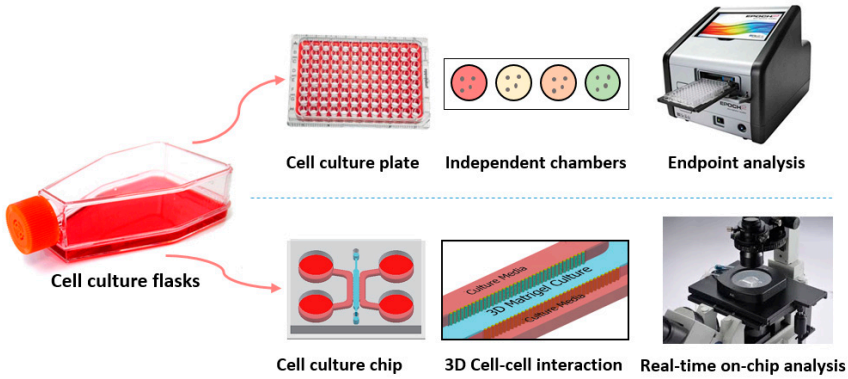

***Figure 1**. Traditional cell culture system and microfluidic cell culture devices.*

Microfluidics makes for a great system for studying cancer cell growth, division, cell mechanics, and cell cycle, in both two- and three-dimensional environments. 3D culture chips have successfully been used to study the complex cellular environment, cell migration and invasion of cancer cells (1). Recently, there have been advances in developing tumor-on-a-chip systems (3) as a new cell culture technology, which integrates microfluidics, tissue engineering and biomaterials to create human tumor models for oncology, immunotherapy studies and drug screening. The model allows well-controlled on-chip-analysis of the interaction among tumor cells, immune cells and tissue.

In addition to cell culture, the capability of studying cell mechanics is another interesting aspect of microfluidics. For example, cancer cells with stiffnesses that differ compared to healthy cells, can be directly characterized in a microfluidic cell squeezer (4) or compressive PDMS chamber (5). By carefully controlling the flow velocities, and visualizing cell morphology using high-speed imaging, it has become possible to measure cellular deformability through real-time deformation cytometry (RT-DC) (6).

Finally, one of the most promising areas of cancer research is the development of a total-analysis-system for separation, culture and analysis of cells on a single device, to enable point-of-care systems. Although there remain several challenges in each method, several successful modular elements have been reported and are

being developed, to combine various functions into a single device as shown in Figure 2.

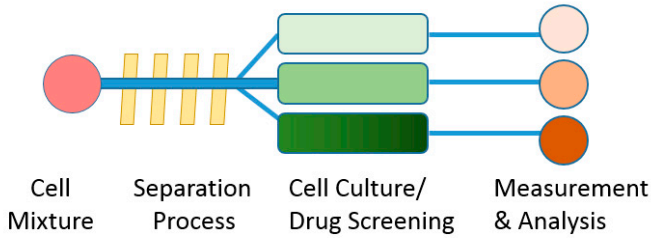

***Figure 2**. Schematic of a microfluidic platform which integrates cell separation, cell culture and on-chip analysis.*

Cell separation in microfluidic devices

Cell separation is an essential preparative step for a vast majority of cell studies. In cancer diagnosis, several conventional cell sorting techniques including centrifugation, chromatography, fluorescent and magnetic-activated cell sorting are currently used. However, these methods have been limited in terms of yield and purity, require expertise in handling, bulky equipment or specific and expensive antibodies. These limitation have fueled the development of microfluidic sorting techniques, which have contributed greatly to the field (1).

The performance of cell separation is strongly dependent on the properties of the sample of interest. The need for isolation and sorting of cells based on different biochemical and biophysical parameters is a central component. For instance, cells can be described by intracellular properties (DNA, RNA, and protein molecule interactions) or extracellular physical properties (size, morphology and surface protein expression). Traditionally, research in the field has used flow-cytometry (7), magnetic separation (8), and density-gradient centrifugation. Novel chip-based technologies have the potential to accelerate discovery and enable sample manipulation to greatly advance the field.

Fractionation of heterogenous biological samples is a major application of microfluidic sorting techniques. Indeed, microfluidic techniques have the ability to separate particles with high precision and resolution in terms of a variety of physical properties and principles (9). These sorting technologies are identified as either

active methods, that apply external forces to sort particles, or passive methods, that exploit channel geometries and hydrodynamic forces including inertial forces (10), obstacle arrays (11), and other mechanisms to achieve the separation.

Another way to categorize these techniques is the need for additional labels: fluorescent label-based sorting, bead-based sorting and label-free sorting. While fluorescent label-based sorting relies on molecular interactions to selectively identify types of cells, label-free separation is based on the inherent physical characteristics of cells. Such physical markers could be size, shape, deformability, density, electrical polarizability, electrical impedance, magnetic susceptibility and hydrodynamic properties.

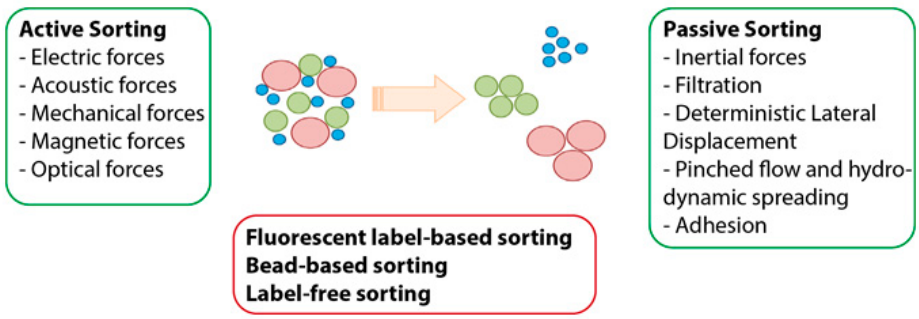

Figure 3. *Microfluidic sorting techniques can be divided into by active and passive sorting methods, fluorescent label-based sorting, bead-based sorting or label-free sorting.*

A short introduction to some of the most popular microfluidic sorting techniques (active and passive methods in the label-free sorting group) is given below. More details could be found elsewhere (12, 13).

- *Pinched Flow Fractionation (14)* separates particles by focusing all particles close to a wall. Based on their size, each particle then follows a separate streamline.
- *Inertial microfluidics (10)* works under specific conditions which maintain both laminar flow and inertial forces to place the particles in different positions within a flow based on their size.
- *Deterministic Lateral Displacement (11)* affects the path of particles through an obstacle or pillar array, based on the particle's effective size and the particular geometry of the array.

- *Field Flow Fractionation* (15) uses an additional force field perpendicular to the fluid flow to separate particles.
- *Acoustophoresis* (16) employs an acoustic field perpendicular to the fluid flow to achieve the separation. Size, density, compressibility are key particle parameters affecting the separation.
- *Electrophoresis* applies an electric field to temporally or spatially separate particles based on their electrophoretic mobility (for instance, gel electrophoresis and capillary electrophoresis (17)).
- *Dielectrophoresis (18)* generates a non-uniform electric field to utilize the difference in size and effective polarizability of particles, and hence enables separation.

From the microfluidic sorting techniques summarized above, Deterministic Lateral Displacement was the technique chosen for the label-free particle sorting presented in this thesis. The technique has been exploited here to separate based on particle deformation and integrated with electrokinetics, in addition to size and morphology based sorting. Furthermore, we present the capability of simplifying microfluidic devices by removing the lid and running them in opening channels. To increase the versatility of the devices, we have explored various ways of tuning the performance.

Deterministic Lateral Displacement: Multiple sorting capability

Adequate resolution, throughput and purity are basic requirements for cell sorting methods. They are also usually used as quality parameters to compare different sorting tools. However, another performance indicator is the number of sorting parameters that can be applied. Deterministic lateral displacement (DLD) is one of a few techniques which is capable of sorting using multiple sample parameters. Key capabilities of DLD are presented in detail in this section.

Passive sorting technique

Deterministic lateral displacement (DLD) is a passive particle separation technique. It was first introduced in 2004 by Huang *et al.* for separation of microspheres by size and DNA by length (11). Using an array of posts or obstacles, the main idea of separation is that the small particles move straight through the device (known as *zig-zag mode*), while bigger particles move with a specific angle (known as *displacement mode*). Figure 4 shows the sketch of a typical device, and demonstrates sorting of polystyrene particles of different sizes in a DLD array.

Due to the micro scale (with the dimensions of channels typically ranging from 100nm to 100µm), the Reynolds number is small and usually less than 500. Therefore, the fluid flow is completely laminar and no turbulence occurs. The sample, consisting of a heterogeneous population, is loaded into an inlet at one end of a pillar array. The particles follow different paths through the pillar array, depending on their sizes: small particles move following the flow in a zig-zag path, while the large particles are displaced relative to the flow direction. The trajectory of each particle is a function of its effective size. The effective size, in turn, is determined by a combination of, for example, size, shape, orientation and deformation of the particles at a certain position.

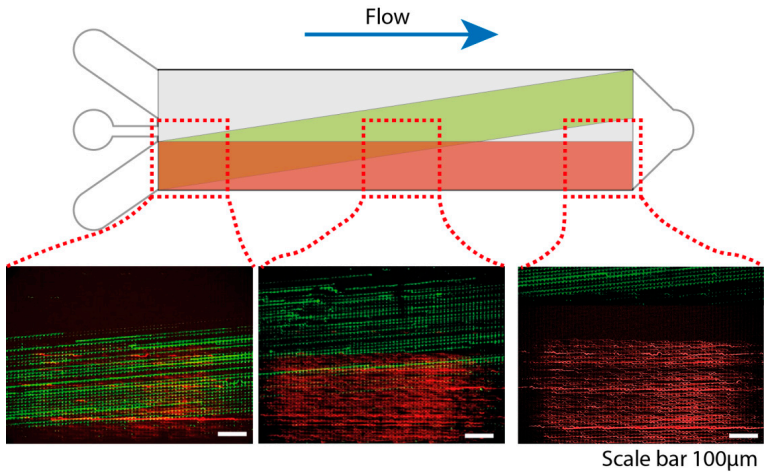

***Figure 4**. Schematic of a typical sorting device along with experimental results. Fluorescence microscopy images show green (diameter: 16μm) and red (diameter: 5μm) particles separated in a DLD array.*

The separation performance of each DLD device is based on the critical size (D_C). Davis *et al*. proposed an empirical formula describing the critical size based on experiments with the circular posts in arrays and rigid spherical particles (19).

$$D_c = 1.4GN^{-0.48}$$

Here, D_C is the critical diameter, G is the gap between two posts, and N is the period of the array. This equation can be expressed in some practical parameters as shown in figure 5.

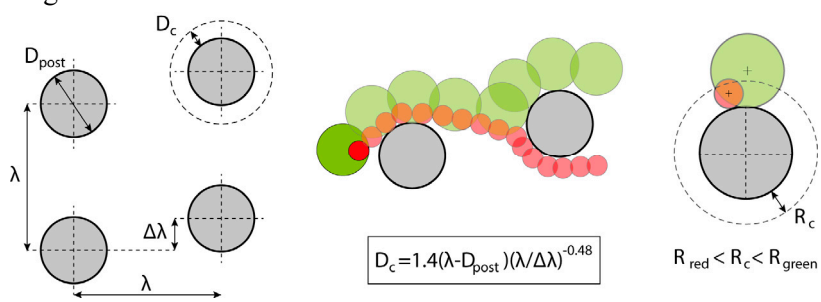

***Figure 5**. Typical definition of DLD parameters and particle behaviors in relation to the critical size. With λ is a space between the post centers, the second row of posts shifted by a distance $= \lambda/N$, where the array repeats itself after N rows.*

The critical size is the most important parameter for the sorting characteristics of a DLD device. Particles smaller than a critical size are defined as small particles, while the others are considered large particles. Besides, gap size and the depth of a device, other device parameters need to be considered carefully for particle selection to avoid trapping and device clogging. Particles larger than the device depth or gap size may be trapped in the reservoirs or in the entrance of the array.

As a passive sorting technique, DLD changes the trajectories of targeted particles, but it does this through the interactions between the particles and the pillar array, instead of due to externally applied fields. This advantage of passive methods makes them less dependent on any additional equipment or skilled personnel and gives a high potential for a portable and easy-to-use tool, for instance, a portable trypanosome sorting tool (20) and open DLD device (21) as shown in Figure 6.

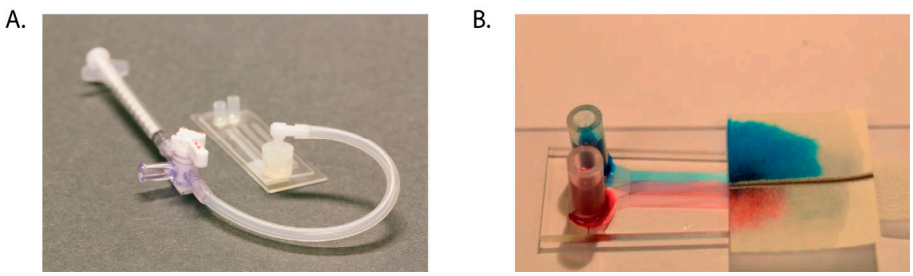

***Figure 6**. Portable DLD devices. A) Trypanosome sorting tool with a handheld syringe. B) Our Open DLD device with capillary flow. Images taken from (20, 21) . Published by The Royal Society of Chemistry.*

High resolution separation

Since the first application in DNA separation and for separation of small polystyrene microspheres (11), DLD has been demonstrated as a high resolution separation technique, with a resolution down to 10 nm. In the last decade, DLD has evolved dramatically and has been adapted to a variety of biological samples with different sample properties. Significant effort has been made to deeply understand the theory as well as design considerations for new target samples. For example, to prevent clogging and to increase the volumetric throughput, much effort has been spent on pillar shape optimization, via both experimental and theoretical approaches. A variety of pillar designs has been reported, including triangles (22-29), squares (26,

30), I- or L-shapes (30-33), diamonds (26), eggs (34), and specific topologically optimized shapes (35) besides circular pillars (Fig.7C). Another consideration is the array design accounting for the wall effect (36), anisotropic permeability effect (37-40) (Fig.7A,B), throughput (24) and combining multiple sections (with different critical sizes) (22).

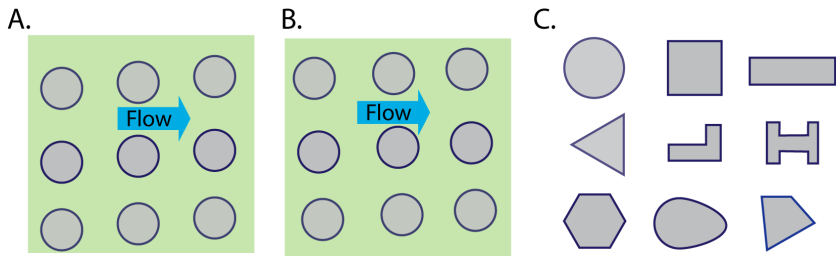

***Figure 7**. Design consideration for DLD geometry. A) Rhombic array B) Rotated squared array with circular pillar. C) A variety of pillar shapes have been optimized for various applications in DLD devices.*

In bio-applications, DLD has been employed to sort a wide range of particles, for instance, fractionation of blood components (12-15), isolation of cancer cells from blood cells (16-18), and parasite separation (20, 41). Other sample types with their sizes are listed in table 1. Among those, the fractionation of blood components is highly interesting. Compared to density gradient centrifugation and direct magnetic approaches, DLD-sorted cells have a more complete and consistent degree of phenotype expression (42). In the near future, automated DLD chips could be a commercial product with precise separation and high throughput (42, 43).

Table 1. Examples of DLD applications in term of particle size and resolution.

	Particle size	**Resolution**
Below 1µm		
DNA length (11, 44)	Bacterial artificial chromosomes 61kb - 158kb (11) Double-stranded DNA 100-10.000bp (44)	~ 90kb ~ 200bp
Exosomes Concentration (45)	Exosomes 20-140nm	~ 90nm
Micro-vesicle from blood (46, 47)	Micro-vesicle 100nm-1µm RBCs &WBCs (6-8µm)	>1µm
Bacteria length (48)	Streptococcus pneumoniae Single Cocci 1-1.5µm Diplococci 3µm, Chain >6µm	>1µm
In a range of 1-10µm		
WBCs from blood (43, 49-60)	Erythrocyte 5-8µm Leukocyte 7-20µm	>1µm
Blood plasma from blood (19, 61-63)	WBCs 5-20µm, RBCs 2-8µm Platelets 1-3µm	>1µm
Nucleated RBC (NRBCs) from blood (64)	Maternal RBCs & Platelets 2µm NRBCs & WBCs 5-10µm	>1µm
Trypanosome from blood (20, 41)	RBCs 2.5-7.5µm Trypanosome cyclops 2.5-30µm	>1µm
Epithelial cells from fibroblasts cells (65)	Epithelial cells 15-20 µm Fibroblast cells 10.7-16.7µm	>1µm
Cardio-myocytes from heart tissue (66)	Cardio-myocytes 7-20µm Non-myocytes 4-71µm	>1µm
Cancer cell lines (28)	SK-BR-3 12.07 µm MDA-MB-231 15.81µm	>1µm

	SUM-159 13.14µm SUM-149 14.13µm MCF10A 14.15µm	
Viable and nonviable Jurkat cells (67)	Viable Jurkat cells 12.3µm Nonviable Jurkat cells 6.9µm	>1µm
In a range of large particles (>10µm)		
Droplet size (68, 69)	Main droplet 61.1µm Satellite droplets 1-30µm Size groups 21.4 µm, 10.1 µm and 4.9 µm	>5µm
Fungal spores from debris (70)	Aspergillus fungal 4µm Spore debris 10-100µm	>5µm
Circulating tumor cell cluster (33, 71-74)	CTC cluster 4-30µm	>10µm

Highly tunable and integrated tool

Although DLD is a size-based sorting technique, its capabilities have been extended to a tunable and integrated device. DLD is also a promising method for sorting based on morphology, density, deformability and surface charge based separation.

In 2011, Holm *et al*. reported DLD as a morphology-based sorting tool in parasite extraction (19). A few years later, Beech *et al.* successfully employed this capability to separate bacteria based on chain length (48). Further, DLD has been employed as a deformability-based sorting tool for red blood cells (23) and platelets (24). Finally, DLD has been used to sort based on density (75).

As a passive method, a fixed geometry design with a specific critical size has limited its flexibility. An attempt of tuning the critical size during the sorting process was proposed by stretching an elastic DLD device (76). However, a complex setting rendered its use impractical. Instead, an integration of electrokinetic forces (77) has proven a clear impact on particle separation, especially for same-sized particles. The implementation complicated the operation of DLD, but it also extended the dynamic range of the device. Another attempt of integration is the open DLD and paper

fluidics (21) that we developed. Ease-of-use in resource limited settings and an open platform for integration are the primary advantages of this method.

Whilst most microfluidic sorting techniques employ a pressure difference to drive the flow and particles, DLD has also been demonstrated with alternative driving mechanisms. For example, capillary force (21, 78), centrifugal force (79), gravity (80) or electroosmotic-driven flow (11, 81) can substitute for syringe pumps or pressure pumps.

In summary, thanks to a vast range of attempts and efforts during the last decade, DLD has been significantly improved with multiple sorting capabilities. With a wide range of applications, it has highly contributed to the particle separation field. This thesis will mainly focus on deformability-based sorting, simplifying DLD fabrication, tunable separation and an open DLD platform.

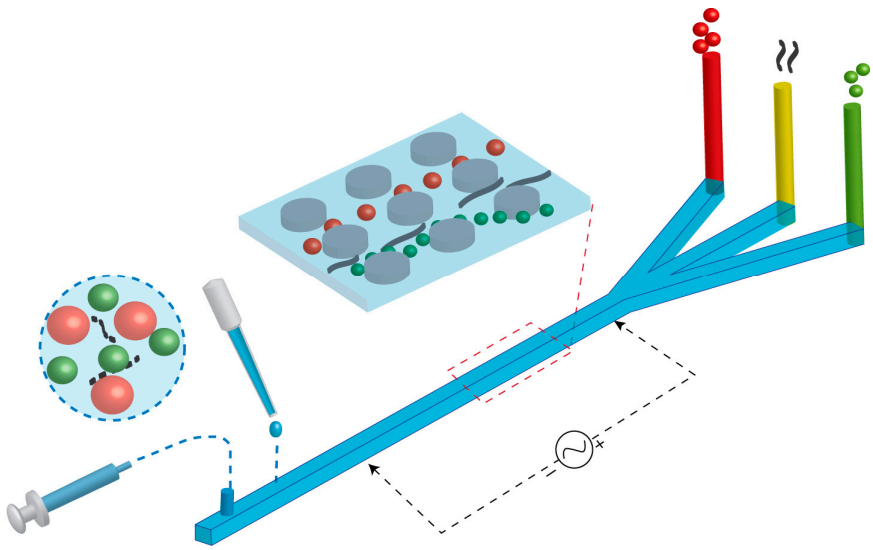

***Figure 8**. Overview of sorting based on size, morphology and deformability. The force driving the flow can be capillary force or applied pressure. Electrokinetic integration is also possible for tuning separation.*

Sample-oriented sorting applications

Size and morphology based sorting

Essentially, DLD is a size-based sorting technique. The difference in size of the particles is the first main consideration for cell sorting. By using an open platform of DLD, we demonstrated size-based sorting for blood fractionation (RBCs 4-8µm and WBCs 10-15µm) and cancer cell isolation from blood (MCF7 cells 15-20µm) (Fig 9A). As the size difference between targeted cells is large (>2µm), the sorting results are clearly observed even without labelling. However, the size parameter may not be sufficient in practice if the particles are non-spherical, such as RBCs (disk-shape) and parasites (long, slender, tapering and arched). Based on the orientation of the particle, the effective size may change significantly. Therefore, an approach of controlling the cell orientation or morphology-based sorting is employed.

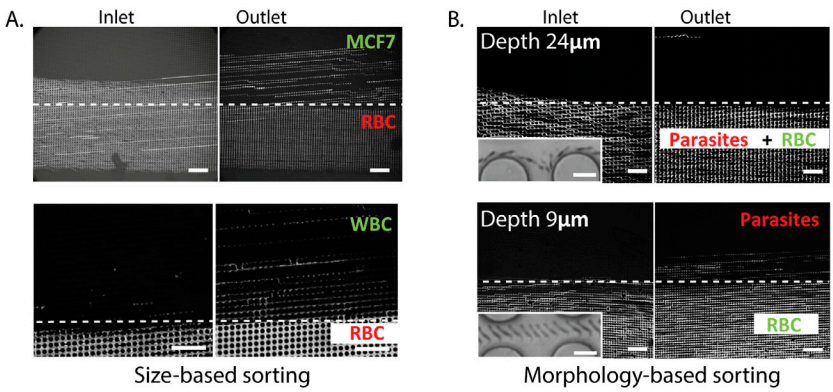

Figure 9. *Size and morphology based sorting for A) cancer cell isolation, blood fractionation and B) parasite extraction. Scale bars 100 µm and 10 µm for the insets. Image from (21), Published by The Royal Society of Chemistry.*

In order to sort out parasites from blood, Holm *et al* (20) optimized the channel height to maximize the displacement of parasites, while RBCs zig-zag. Figure 9B

presents the effect of channel height in relation to parasite flow-behavior. As illustrated in the figure, no parasites are isolated in a device of depth 24 µm, while in a 9 µm deep device, all parasites displace to an upper stream. However, the shallow channel reduces the volumetric flow rate, and thus the throughput or parasite capture rate. In an attempt to orient RBCs without modifying the channel geometry, electrokinetic forces may be superimposed to induce rotation of RBCs in the flow.

Dielectrophoresis – an external field

In 2009, Beech *et al.* (77), introduced dielectrophoretic forces in the pillar array. The use of dielectrophoresis (DEP) has paved way for particle separation based on polarizability, in addition to hydrodynamic size, in the DLD devices. By changing the frequency and magnitude of the applied electric field, the effective size of the particles is tunable, and hence separation is possible. As an alternative to fabricating DLD devices with the specific depth to obtain the parasite extraction, we explore how the effect of the DEP force or other electrokinetic effects may help separation in this study.

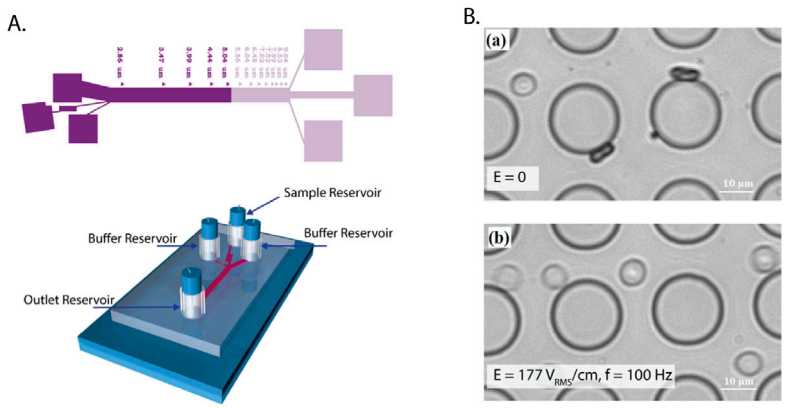

***Figure 10**. Experimental setting and results A) Electrodes attached at inlet and outlet reservoirs in a DLD device B) The orientation of RBCs as a function of an applied electric field (at 100Hz). Scale bar 10 µm.*

Although the rotation of RBCs was observed clearly and the displacement was achieved, high voltages were required and, there was an issue of cell viability due

to Joule heating. Since PBS buffer has a high electrical conductivity (1660mS/m), the temperature may increase significantly when high voltages are applied. An attempt of reducing medium conductivity by sucrose showed a better result of cell morphology (compared to the spherical shape of few cells in the high medium conductivity) while cell displacement was decreased. Further optimization of the running medium to maximize RBCs rotation is required for successful use of the approach for parasite extraction from blood.

In the closed DLD devices as mentioned above, electrodes may only be placed externally in the inlet and outlet reservoirs, which leads to relatively low field strengths in the array. In order to maximize the external force, introduce flexibility of the localization of the stimulated area as well as reduce the Joule heating effect, the open DLD platform has been investigated.

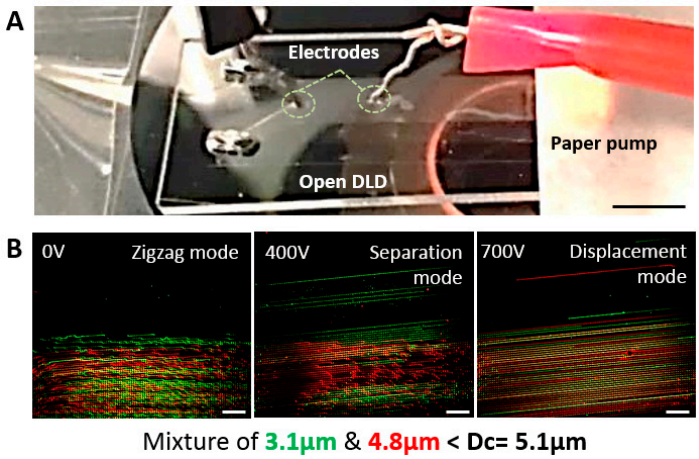

Figure 11. *Combination of open DLD and Electrokinetic DLD. A) A typical set up where electrodes are placed in the selected area. B) By tuning the applied voltage (0V, 400V and 700V), the trajectories of particles are changed. Scale bar 100 µm. Images taken from (21). Published by The Royal Society of Chemistry.*

In the experiment (Fig.11), a mixture of 3.1 µm and 4.8 µm microspheres were separated in a DLD device (*Dc*=5.1µm). The separation was obtained at 400V. The result was similar to the closed device but the applied voltage was smaller and occurred in a smaller zone. Other advantages of open microfluidics will be discussed in the open DLD section. As a short conclusion, the external force, in this case dielectrophoresis, has expanded the sorting capability of DLD and thus demonstrates a useful integration of two mechanisms in the device.

Device deformation for tunable separation

Many sorting problems require optimization for a successful result. We have approached this problems in two ways: a combination of electrokinetics with DLD for tuning RBCs rotation or tuning particle separation in the open platform or through the deformation of the DLD devices by control of the driving pressure. The second approach of device deformation is expressed in this part.

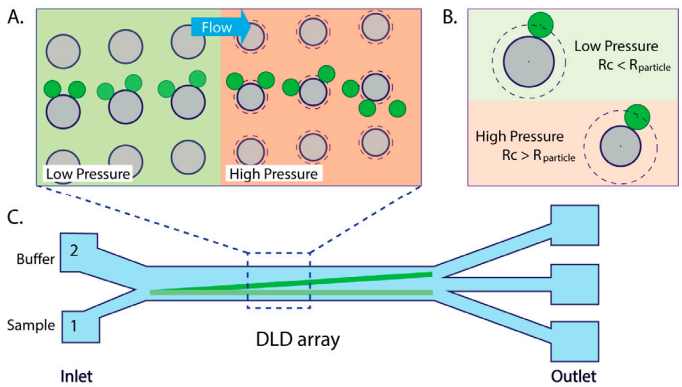

***Figure 12**. Effect of soft pillar change on particle distribution. A) DLD array and particle trajectories in low and high pressure. B) Critical radius and particle size in both cases. C) A schematic of a DLD device.*

Figure 12 shows the effect of post deformation on the particle trajectory. High applied pressure causes the post compression and decreases its size as well as increases the critical size of the array (following the Davis's equation (19)). As a result, the particles which are expected to displace (due to the effective size being larger than the critical size) now move in the zig-zag mode (effective size smaller than the critical size).

In our experiments, 15µm Polystyrene beads were used to calibrate the device as shown in figure 13. When the driving pressure is increased, the particles shift to the left and assume to a smaller value of the effective size. Due to the high stiffness of the beads (Young's modulus of 3-3.6x10^9Pa), the deformation of PDMS is considered and taken in account for a correction. In paper 5, a correction of the critical size is performed by the measurement of post deformation.

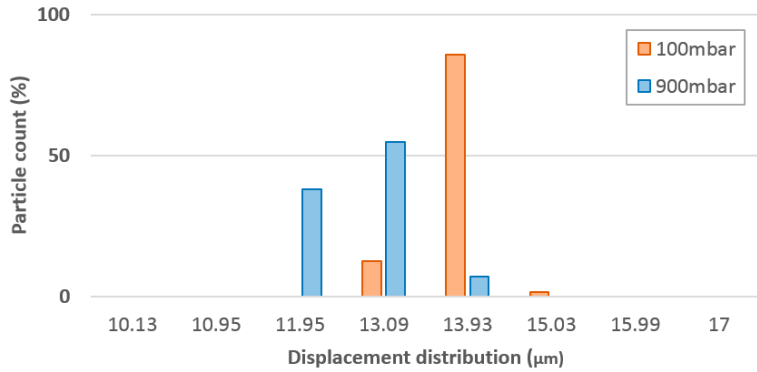

***Figure 13**. A comparison of 15μm Polystyrene beads at low (100mbar) to high pressure (900mbar). The displacement distribution was effected by pressure control.*

The deformation of the posts is related to the stiffness of PDMS which in turn depends on the mixture ratio (the base and the curing agent) and curing time and temperature. The deformability of the device also depends on how much material is deformed and so the Device thickness is also important. A survey of these parameters is shown in figure 14 (curing time has not been tested yet). In this survey, we test different combinations of parameters for PDMS device fabrication in order to avoid or exploit the deformation.

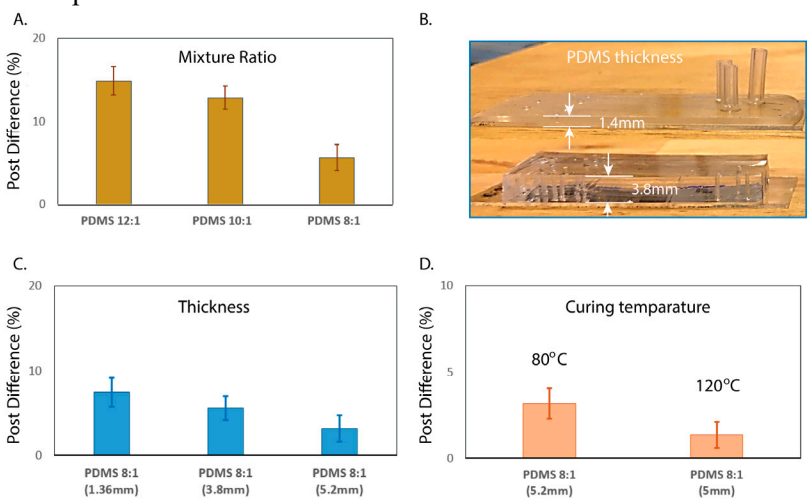

***Figure 14.** Different parameters related to PDMS stiffness. A) Mixture ratio (12:1; 10:1 and 8:1). B) &C) Device thickness (1.36mm, 3.8mm and 5.2mm) and D) Curing temperature (80°C and 120°C). Post difference refers to the relative change of the post diameters upon application of a 900mbar pressure across the device.*

Deformability as a marker for cell sorting

Deformability

Size and morphology are basic label-free markers which are commonly used to discriminate cell types and effectuate separation in DLD. However, in this section, we discuss the mechanical property of deformability as an additional separation parameter. We aim to exploit deformability as a biomarker, to identify cell types as well as to separate them. The aim is cancer cell detection and isolation for cancer cell analysis and diagnostics.

In general, cancer cells are derived from normal healthy cells and undergo uncontrolled growth and division. Although cancer cells have a wider size distribution than their healthy counterparts, and may also have higher prevalence of irregular shapes, the significant overlap in these characteristics renders them unusable as distinguishing or separation parameters.

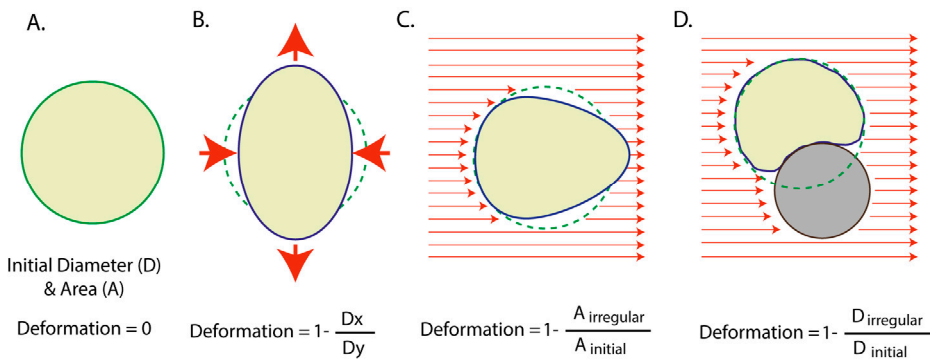

***Figure 15**. Different approaches for deforming a spherical particle along with different definitions of deformation.*

We examined a breast cancer cell line (MCF7) and normal cells (MCF10A) in suspension using optical microscopy. Without labelling, the two cell lines are indistinguishable. Size and shape measurements give a better understanding of the similarities. While the breast cancer cells have a wide size distribution, which overlaps with the distribution of normal cells (15.5±4 µm and 15.1±2µm, respectively), the circularity shows a uniform spherical shape of both cells. A significant difference between the two cell types is their propensity to form

aggregates; 12 % of the cells form aggregates for MCF7 and 3% for MCF10A. It is believed that cancer cells prefer to form aggregations or clusters (82).

In cancer cell research, higher deformability has been shown to be an inherent characteristic of metastatic cells (83). Without the need for chemical modification or molecular labelling, deformability is a label-free biomarker, has potential as an important parameter for cell characterization and cell phenotype discrimination. To measure the deformability of cells, a variety of techniques have been reported, such as micropipette aspiration (84), atomic force microscopy (AFM) (85-88), optical tweezers (89), and real time deformability cytometry (RT-DC) (6). By stretching or compressing a single cell in the optical tweezer (83) and AFM (85), a spherical cell is deformed into an ellipsoidal shape as in figure 15B. Each single cell will be independently measured and evaluated with respect to its degree of deformation. RT-DC, was introduced in 2015 by Guck *et al*. RT-DC has a much higher throughput (100 cells/s) (6). In a micro-channel, images of single cells are captured using a high-speed camera. Shear forces cause cells to deform into a bullet shape (Fig.15C). The shape of the deformed cell is used to calculate its deformability. An alternative method is a ratchet method (90), which traps cells in microfluidic constrictions, an effect that depends on deformability.

DLD and cell deformation

We aim to employ deformability as a label free marker for cell sorting in the DLD array, where the effective sizes of particles determine their trajectories and outlet distributions. Figure 16A shows how the effective size of a particle can change with deformation and how this can have a large effect when the effective size becomes equal to the critical size. Particles larger than the critical size, R_C, will displace while the others follow the flow. In the case of soft particles, although particle size is larger than the critical size, the effective size could be smaller (due to the deformation) and they behave like small particles (Fig.16B).

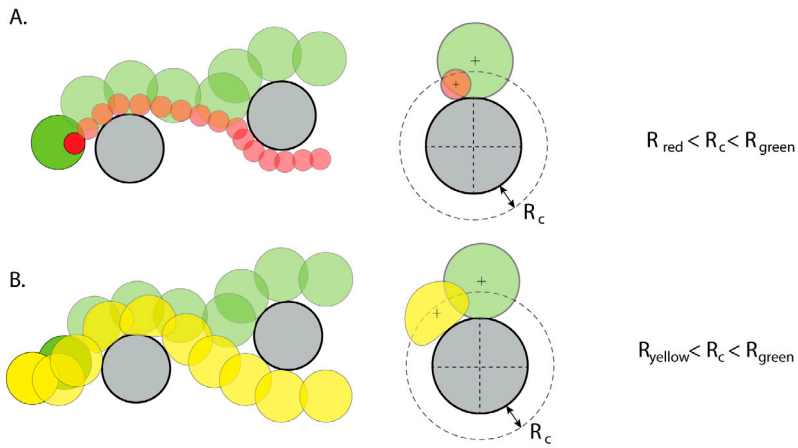

***Figure 16**. Particle trajectories in relation to size, and deformability. A) Both hard particles with size difference. B) Same-sized particles with difference of deformability.*

Different cell types have been shown to undergo different ranges of deformation (83, 86). As an example of cell deformation, an individual MCF7 cell was captured at high driving pressure (900mbar) in figure 17A. At low shear rates, the small (red) cells are in zig-zag mode and the large (green) cells are displaced following the DLD sorting mechanism. At high shear rates, the large cells deform (yellow) move in the zig-zag mode, together with smaller cells.

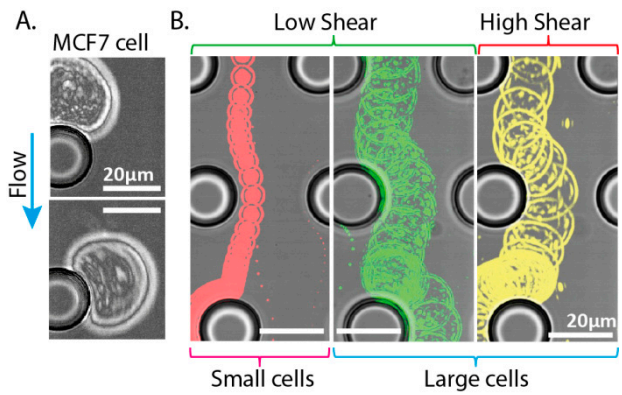

***Figure 17.** Cell deformation in a DLD array. A) MCF7 cell deformed at high pressure (900mbar). B) Based on size and deformability, different trajectories of cells are observed.*

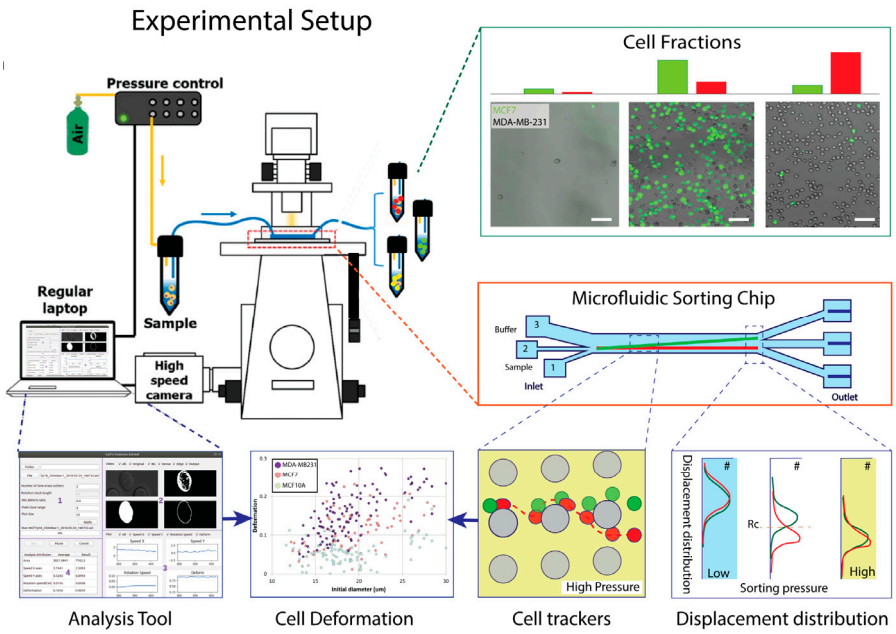

Figure 18. *Overview of deformability-based sorting experiment. A sample of cells was loaded into a microfluidic sorting chip (DLD) by air pressure (controlled by the users). During the sorting operation, the sample could be captured in different selected areas for the measurement of cell deformation, cell tracking or cell counting. An analysis tool was used to detect and extract all needed information to obtain the results (the single cell measurement, the displacement distribution or the sorting purity). After sorting, different fractions of cells were collected and used for downstream analysis. Scale bar 100μm.*

Figure 18 gives an overview of our work on the deformability-based sorting for cancer cell characterization and isolation. The cell identity and deformation have been characterized at three distinct levels.

- Firstly, single cells are directly visualized when in contact with the post array. The deformation is extracted using an image analysis tool developed for the purpose.
- Secondly, cell distributions at the end of the array are counted and measured. The deformation is inferred from the position of the cell at the end of the device. A different image analysis method is utilized for this approach.
- Finally, different sorted fractions are analyzed at the outlet reservoirs to confirm the sorting capability.

In summary, we have successfully demonstrated and measured the deformation of non-malignant cells (MCF10A), breast cancer cells (MCF7) and invasive cells (MDA-MB-231) using DLD devices (Paper 2). We find that the invasive cells (MDA-MB-231) are highly deformed at the high flow rates (900mbar) while MCF10A cells are slightly deformed compared to MCF7 cells. While the direct visualization of the cell deformation process gives better values on deformability (since both the size and deformation are simultaneously measured for individual cells at high magnification and resolution) (Fig.19A & B), the second approach allows the measurement to be performed on many more cells but gives less accurate results (measurements are done at much lower magnification and resolution) (Fig.19C & D). The first approach is limited by the amount of data that can be collected for each cell which in turn is limited by data transfer rates and the internal memory of the camera. As a result, the data only represents a small number of cells (less than a hundred cells for each cell line).

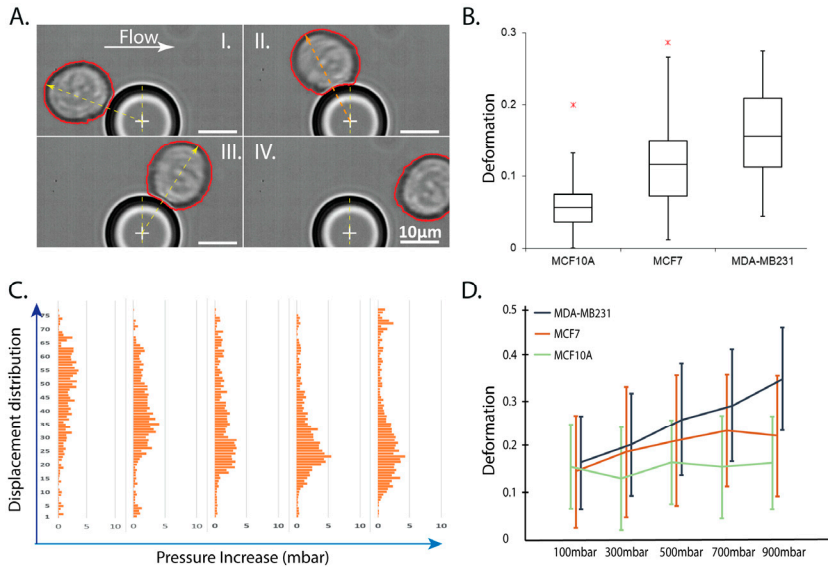

Figure 19. *Cell deformation among three cell lines (MCF7, MCF10A and MDA-MB-231). A) &B) Direct measurement from image features (at 900mbar). C) & D) Indirect measurement from cell size and displacement position.*

In this section, we propose the use of a DLD device as a deformation measurement tool, besides its separation capabilities. By optimizing the data processing and hardware setting, it is possible to develop a real-time analysis and sorting system, for cancer cell analysis and diagnosis.

To test cell separation, a sample of cells is loaded to the DLD array. Based on the correlation between displacement distribution and applied pressure for each cell line, matching data helps us to identify the sufficient pressure which maximizes the sorting efficiency. For an example of matching data, a comparison of stained MCF7 and MCF10A is shown in figure 20.

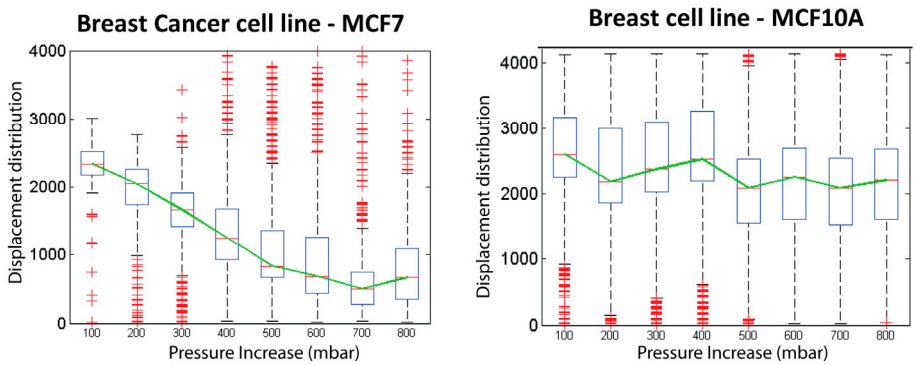

***Figure 20**. A comparison of displacement distribution of stained MCF7 and MCF10A cells. The mean value of the box-plot presented two different tendencies of cell distribution in relation to pressure increase (from 100-800mbar). The outliers showed the distribution of very large or very small cells. As a results, the separation between two kinds of cells could be obtained from 400mbar.*

Another mixture of MCF7 and MDA-MB-231 cells was passed through the DLD array. Because the high speed camera used in these experiments was not sensitive enough to visualize fluorescence from cells moving at high flow rates through devices, it was not possible to visualize displacement distributions. Instead, we collected cells in containers at the outlets of the device and then counted the cells post separation (Fig 21).

The ratios of the different cells types in the collection tubes shows a significant difference compared to the initial mixture (50:50). In tube 2, the ratio reached 71:29, (MDA-MB-231:MCF7) and close to 75% of MDA-MB231 cells were collected. In tube 3, the ratio of was 32:68, and close to 35% of MCF7 cell were recovered.

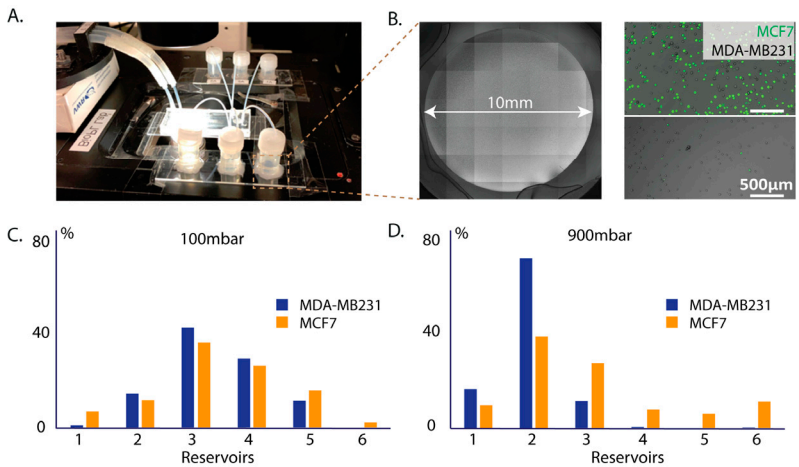

Figure 21. *Deformability-based sorting for MCF7 and MDA-MB-231 cells. A) A typical setup for cell sorting. B) Tube reservoir in a large scale and fluorescent images to distinguish MCF7 (GFP) and MDA-Mb-231 cells. C) Percentage of cells in each tube at 100mbar. D) The separation occurs when MDA-MB-231 cells deforms more than MCF7 does.*

Although the performed separation does not demonstrate high purity, the results clearly demonstrated the effect of cell deformation on the sorting process. Future work in this direction would aim at a new design of DLD with smaller critical size, and higher operational pressures.

Challenges

While the above sections have described the potential of DLD and other microfluidic sorting techniques, in practice, there exist several challenges to be considered as clogging, high throughput application, easy-to-do operation or mass production of devices.

Clogging is a common issue when loading particles in a micro-channel (91) and pillar array can be especially susceptible to this. In a common DLD device, there is a large surface area where particles will interact with posts and walls. The interaction commonly causes clogging during device operation. We studied the ability of different surface treatments (PLL-PEG, Pluronic, and BSA) (92) to prevent clogging. In some cases, we can used adhesion in the sorting process, see the section of open DLD below with the application of blood purification.

Simplifying microfluidic separation devices

Open channel approach

To simplify the microfluidics, we have explored a DLD device without a lid on the microfluidic channels. We have demonstrated the advantages of accessibility (addition of reagents, retrieval of biologic liquids or objects, human intervention on the system), the minimization of air-bubbles and clogging and how the open architecture facilitates cleaning. We expect that open microfluidics (93) to be a potentially highly interesting choice for point-of-care and home-care-systems.

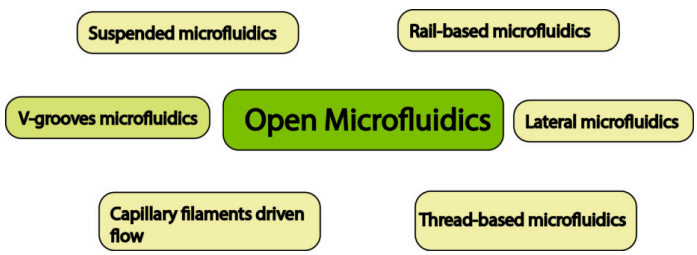

Figure 22. *Overview different open microfluidics that has been reported in the literature.*

The first open DLD, introduced at MicroTas 2009 (78, 94), showed a successful result of separating the small particle from the mixture by capillary flow. The improvement of separation (for both small and large particles), sample volume and continuous flow was done by our work a few years later when an integration with paper fluidics was utilized successfully. A complete device with varying bio-particle sorting applications was presented recently in Paper 1 (21). The open DLD chip is a portable tool with good prospects to use outside the lab and in resource deprived areas.

To realize the open DLD we simply remove the lid of a typical DLD chip, treat the surface, add reservoirs in the inlets and paper channels at the end of the array (Fig.23). A complete open DLD device contains a PDMS stamp, two inlet reservoirs, and an additional paper capillary pump with wax lines. For practical use, the sample and buffer are loaded separately in two inlet reservoirs of a pre-wetted PDMS device. The reservoirs allow us to load the device with more sample than if we had we just added the sample as droplets on the surface. By the capillary flow and the sorting mechanism in the DLD array, the sample is sorted into different fractions and collected by the paper. Figure 23A presents the entire process of sorting in an open DLD device. When the sorted fractions stay in the paper, a downstream analysis could be directly conducted or a process of particle extraction could easily be done by vortexing the paper to release the sample. The function of the paper will be explained below.

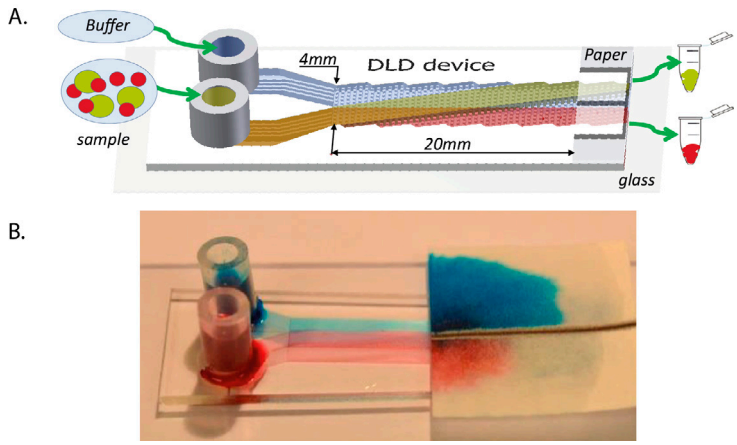

***Figure 23**. A) An illustration of particle sorting in an open DLD chip. B) A typical device with food colors to present the laminar streams. Images taken from (21). Published by The Royal Society of Chemistry.*

A characterization of the liquid profile along the device could be found in three experimental approaches: a macro photography image of the liquid inside the DLD array, a confocal image of 3D liquid volume and a study of the flow in the channel. The results give a better understanding of the flow inside the open DLD channel and confirm that the fluid is confined in an open channel (21). Overall, open channel DLD with new components (reservoirs and paper) are easy to assemble and easy-to-use with particular relevance to applications in resource-poor settings.

To test biological applications, we demonstrated the open DLD technique for a range of mixtures of samples in several different sorting schemes. As a powerful mechanism for size-based sorting, traditional DLD and open DLD perform similarly for blood fractionation (RBCs and WBCs) and cancer cell isolation (MCF7 and RBCs). Figure 24 presents a typical setup of sorting MCF7 from blood and trajectories of two kinds of cells were observed without fluorescence. The RBCs are prevalent at a higher concentration than the MCF7 cells so they can easily be visualized in the paper. To evaluate the purity of sorting, fluorescent dyes were added to both cells in a different experiment (Figure 7 in Paper 1). Morphology-based sorting is another promising aspect of DLD applications. In this study, Trypanosomes were isolated and enriched from RBCs in an open DLD device with depth 9µm. In another example of open DLD we sorted single cells from clusters of MCF7 cells. A summary of the cell sorting in open DLD is found in figure 24C.

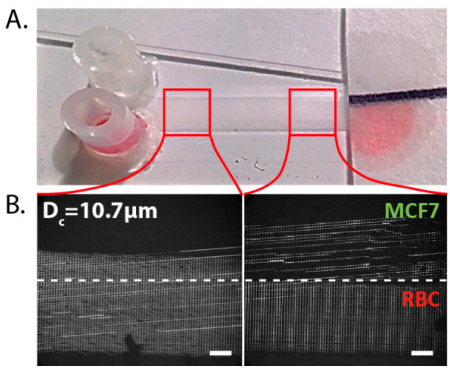

C.

Open DLD	Cell Sorting
Device 1 (Dc=5.1µm)	RBCs and WBCs
Device 2 (Dc=10.7µm)	RBCs and MCF7
Device 3 (Dc=14.5µm)	Single and Clusters MCF7
Device 4 (Dc=5µm, depth 9µm)	RBCs and Trypanosomes

***Figure 24**. Cell sorting in open DLD chip. A)&B) Sorting MCF7 from blood.C) List of devices and bio-applications. Images taken from (21). Published by The Royal Society of Chemistry.*

An additional advantage of open devices is the ease with which they can be cleaned and reused. A closed DLD device, which is sealed to prevent leaking, is hard to clean and reuse when clogging takes place (Fig. 25A and B) while an open device can potentially be reused after a simple cleaning step (Fig. 25C).

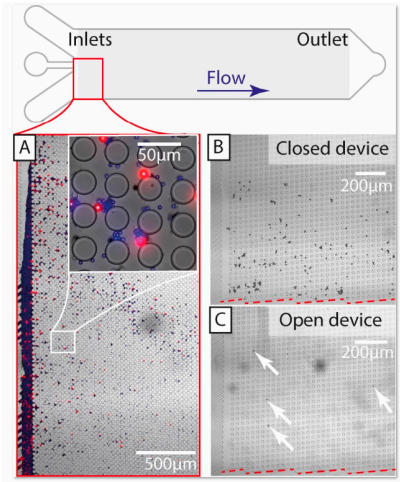

***Figure 25**. Cleaning and reusing an open DLD chip. A) Clogging in a device. After washing in B) Closed device and C) Open device. Images taken from (21). Published by The Royal Society of Chemistry.*

In some cases, the adhesion issue could give a benefit for particle sorting. For an example of forensic cases, RBCs and WBCs need to be separated from contaminated blood samples including soils and dust (Fig.26). Due to the small contaminant sizes, they cannot be filtered out by a filter membrane. Instead, a DLD array having two roles has been tested. The first array traps the contaminants, while the second one is used to sort the remaining RBCs and WBCs. With a negative charge of the PDMS surface, the small sized soil and dust particles were trapped in several first rows, while RBCs and WBCs pass through this section to be continuously sorted according to the main function of DLD.

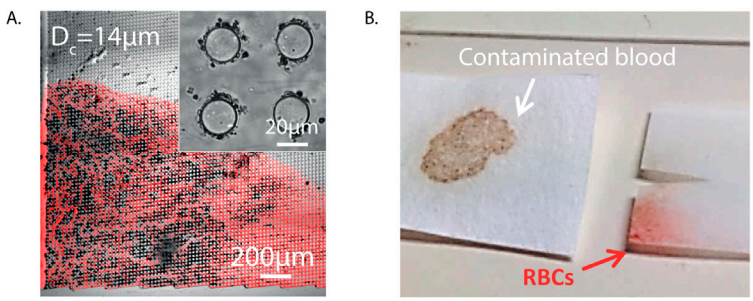

***Figure 26.** Contaminated blood is purified by passing through the array. Images taken from (21). Published by The Royal Society of Chemistry.*

We have successfully demonstrated that open channel DLD devices assembled with capillary paper pumps are promising portable tools for particle and cell sorting. In terms of size-based sorting and morphology-based sorting as well as potential to integrate with other techniques, such as electrokinetics and paper fluidics, we have shown that open channel DLD has the potential to open up for new applications.

Paper fluidics

As a passive technique, DLD is an open platform to integrate or combine with other techniques in a whole system. Here, we exploited the capability of both closed and open DLD chip as an integrated and tunable platform.

As mentioned above, the paper plays an important role in an open DLD system. The paper provides a good solution to maintain a continuous flow, which is important to achieve a continuous sorting. As a capillary pump, the paper contributes a negative pressure to increase and stabilize the flow rate (95-98). A study of the flow rate in the open channel DLD as well as in the paper with evaporation taken into account was conducted in different experiments. Compared to the flow driven by the capillary wetting of the paper, the flow due to the hydrostatic pressure of fluid in reservoirs and the absorption rate of paper are significantly less in magnitude. With a paper fluidics geometry that allows the sample to wet the paper in a semicircle or half a semicircle the resulting flow is essentially constant.

Another aspect of paper fluidics is that it is an attractive substrate for various biomedical applications. Paper based lateral flow tests without the need for specialized and costly equipment are commonly used for medical diagnostics, POC tools and home-care testing. Furthermore, paper-based cell culturing has been developed as a promising approach that allows cells to grow in both 2D and 3D cultures. In this study, paper was used as a convenient substrate that is easy to collect, transport or release the sorted sample from in order to pass it to subsequent analysis. In practice, after sorting particles in an open DLD, the paper is cut out into different fractions. The isolated particles are released into suspension by vortexing and collected by spinning (Fig.27).

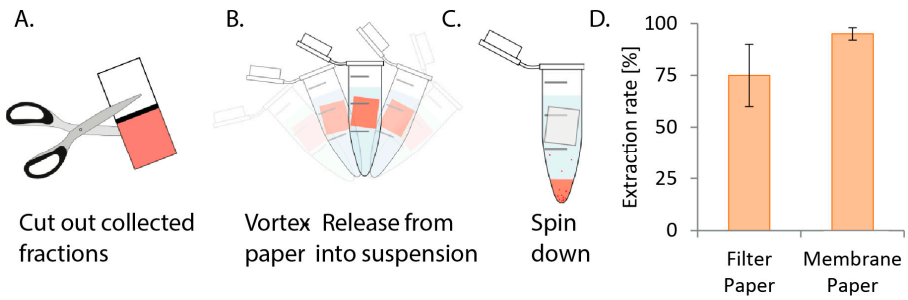

***Figure 27**. Sample collection from paper fractions. Images taken from (21). Published by The Royal Society of Chemistry.*

Various types of paper with different pore sizes, retentions and materials were tested in terms of absorption rate and sample extraction rate. Among these, a filter paper with a good absorption rate was selected for use as a capillary pump and a sandwich paper (filter paper and membrane paper) was applied to increase the sample extraction rate. A comparison of extraction rates is shown in figure 27D. In future work, a bio-compatible paper for cell culture or lateral flow paper could be utilized in the open channel DLD substrate for integrating a series of POC tools.

Device fabrication and sample preparation

Glue-based mold and multi-layer device

From the initial design to a complete device, the fabrication of a microfluidic device is a long procedure with several steps, including design consideration, simulations, fabrication and verification. The process can be resource-intensive, relying on *e.g.* design software, UV-lithography, plasma chamber. In an attempt to reduce the processing effort in soft-lithography and to increase device throughput, we propose a rapid duplication method for PDMS devices in single layers as well as stacks of multilayers.

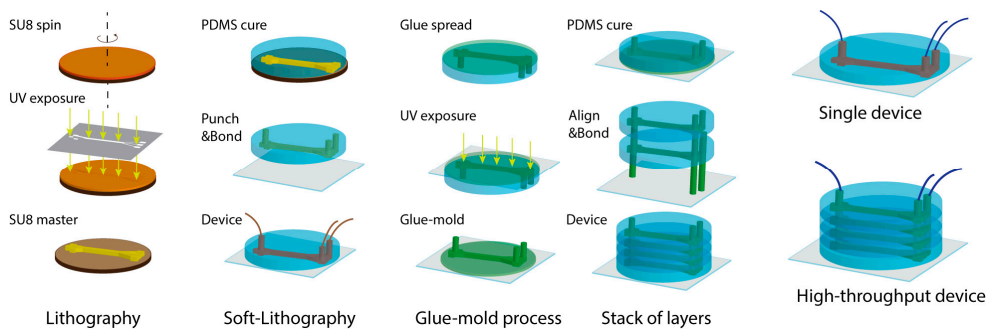

Figure 28. *Traditional process of single device fabrication (Lithography and Soft-lithography) and additional method for a stack of layers (glue-based mold and alignment).*

Figure 28 shows a brief summary of the device fabrication process which is mainly based on the lithography and soft-lithography processes. In order to protect and extend the lifetime of SU master, a novel method to create a secondary mold has been developed. In our work, a secondary mold made of UV-curable glue is introduced instead of PDMS (99) or Epoxy materials (100), with the advantage of high-resolution replication and no need of anti-sticking treatment.

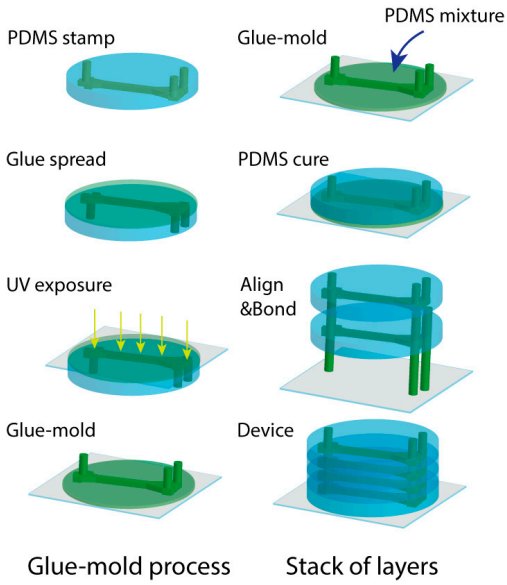

Figure 29. *Process of glue-based mold fabrication and alignment step of a stack of layers.*

A PDMS stamp duplicated directly from SU-8 master was used to fabricate a secondary mold in the process (Fig.29). After curing, a glue-based mold is used for PDMS replicas. Furthermore, a new approach based on alignment pins for quickly aligning PDMS multilayers is simplifying the process of making a high-throughput devices (Fig.30).

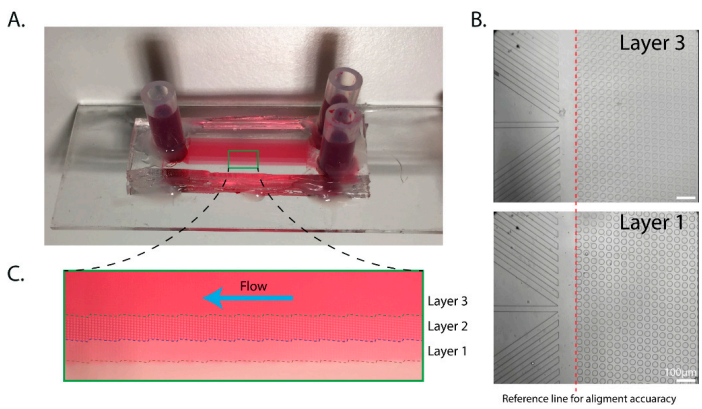

Figure 30. *A) A three-layer DLD device with food color. B) Optical images of first and third layer in different focus plans. C) Three layers of devices were observed through the red color. Scale bar 100µm.*

PDMS device fabrication

The masters for the DLD arrays were fabricated via UV lithography. In a contact mask aligner (Karl Suss MJB3 and MJB4, Munich, Germany), negative photoresist SU8 (MicroChem, Newton, MA, USA) spun on a 3" silicon wafer was exposed to UV light through a chrome-mask designed in L-Edit 11.02 (Tanner Research, Monrovia, CA USA) and printed by Delta Mask (Delta Mask, Enschede, The Netherlands). Before casting of PDMS, a monolayer of 1H,1H,2H,2H-perfluorooctyl trichlorosilane (ABCR GmbH & Co. KG, Karlsruhe, Germany) was applied in the gas phase to the master as an anti-adhesion agent to facilitate demolding. A 10:1 mixture (monomer : curing agent) of PDMS (Sylgard 184, Dow Corning, Midland, MI, USA) was degassed, poured onto the master and then baked for 2 hours at 80°C.

For the closed devices, PDMS stamps are punched and an oxygen plasma treatment step (Plasmatic Systems, Inc., North Brunswick, NJ, USA) is performed to enable bonding to glass slides. Silicone tubes for fluidic connections are glued to the device with silicone glue (Elastosil AO7, RTV-1 silicone rubber, Wacker Silicones, Munich, Germany).). For the open device, the PDMS stamps are directly assembled with a paper pump, with or without reservoirs. A comparison of the protocols of the two fabrications is presented in Supplementary of paper 1 (Open channel DLD for particle and cell sorting).

Paper fabrication

Single and two-layer paper systems were used as capillary pumps and for sample capture and collection. For liquid absorption (Herzberg flow rate 110sec/100ml), a filter paper of 0.15mm thickness, a 25-60µm pore size and 8µm particle retention (Grade 600, VWR, Sweden) was used. For sample capture, a layer of polycarbonate paper (Grade 28158, VWR, Sweden), (0.1µm pore size) was sandwiched between the separation device and the lower grade filter paper. Wax barriers were printed onto the filter paper using a wax printer (ColorQube 8570, Xerox, USA) followed by baking for 3 minutes at 100° C.

Sample preparation

Fluorescently labelled polystyrene microspheres with varying diameters (from 1µm to 20µm) (Polyscience Inc.) were suspended in milliQ water and 1% SDS, and used in both closed and open DLD devices for calibration.

Soft polyacrylamide particles (diameter 15 ± 0.84µm, Young's modules 670 ± 280 Pa) obtained from Prof. Guck's lab (TU Dresden, Germany) were used as particle reference in softness sorting in DLD (101).

Small volumes of blood (10 µl) were obtained from healthy, consenting donors via finger pricking. Blood samples were diluted 20 times in autoMACS™ running buffer (Miltenyi Biotech, Auburn, CA).

Trypanosoma cyclops parasites were thawed (after storage in 10% dimethyl sulfoxide (DMSO, Fluka, St Louis, MO: 41639) at -80°C) and cultured in Cunningham's medium 15 with 20% Fetal Calf Serum (FCS, Sigma-Aldrich) at 28ºC. Parasites were harvested after proliferating to cover 80% of the culture dish and spiked into blood samples.

MCF-7 (breast carcinoma cell lines obtained from the American Type Culture Collection (ATCC)) was cultured at 37°C and 5% CO2. Cell culture medium was DMEM, 10%FBS and 1% Penicillin-Streptomycin (Sigma-Aldrich). MCF-7/GFP (breast carcinoma cell lines with Green Fluorescent Protein) (NordicBioSite) was cultured using the same protocol as the non-fluorescent MCF7. MDA-MB-231 (metastasis breast cell lines obtained from the American Type Culture Collection (ATCC)) was cultured at 37°C and 5% CO2 in a culture medium comprising of DMEM, 10%FBS and 1% Penicillin-Streptomycin.

MCF-10A (human breast cell lines obtained from the American Type Culture Collection (ATCC)) was cultured at 37°C and 5% CO2 in a culture medium comprising of DMEM, 5% Horse Serum, 20ng/ml Epidermal Growth Factor (EGF), 10ug/mL Insulin, 0.5ug/mL Hydrocortisone, 100ng/mL Cholera Toxin and 1% Penicillin-Streptomycin (Sigma-Aldrich). After one week of culturing, cells reached confluency of approximately 85-90% and were considered ready for separation experiments.

Image Acquisition and analysis

Particle and cell distributions were calculated from images acquired using an inverted epifluorescence microscope (Nikon Eclipse Ti, Nikon Corporation, Tokyo, Japan) and scientific CMOS camera (Flash4.0 V2, Hamamatsu, Japan).

A high-speed camera (MotionBLITZ Eosens mini, Mikrotron GmbH, Unterschleissheim, Germany), capable of capturing 10.000 frames per second, was used to obtain images of the particles and cells at high flow rates (>100ul/min).

ImageJ 1.48v software downloaded from the National Institutes of Health, and NIS-elements 4.51 were used for basic image analysis and the preparation of several of the figures herein. Images of particle trajectories were generated by time-averaging and two-color images generated by adding color to separate images, taken in succession with different filter sets, and superimposing.

Matlab R2014a software was used to write the image analysis code for the specific needs of cell detection, counting and morphology detection.

All error bars of data shown in graphs and figures were calculated by average values and standard deviations of repeated experiments.

Summary of results and outlook

In this thesis, we successfully introduced the open DLD, a portable tool for particle and cell sorting with the capability to sort out various biological samples in terms of size and morphology without external equipment. It was proposed as a potentially useful device for conditions at resource-poor settings. The open DLD method can be further developed and put to use by integrating a reliable downstream method for identification of the sorted cells, for instance paper fluidics with specific antibodies to realize a lateral flow diagnostic device.

In another example of cell sorting, we demonstrate that deformability can be an interesting bio-marker, especially when size and morphology based sorting are not sufficient to extract the specific cancer cells of interest. We have also introduced cell deformation measurements in DLD devices. The results show a significant difference of deformability among cell lines of MCF7, MCF10A and MDA-MB-231 cells. A proof-of-principle of cancer cell sorting using MCF7 and MDA-MB-231 cells is illustrative for deformability-based sorting using DLD. However, the work on isolation of cancer cells from the normal cells is still not yet finished. Furthermore, a comparison of DLD and FACS will give a better understanding of cell characteristics. In future work, more relevant cancer cells, *e.g.* clinical samples, are planned to be sorted using our techniques. To characterize the metastatic potential of the different sub-populations of the cells, transplantation of the sorted fractions in terms of size, morphology, deformability will be explored. To better understand and predict deformability sorting, better theories need to be developed.
Two approaches of tuning cell separation have been introduced in different applications: a combination of electrokinetics and DLD for tuning RBCs rotation and device deformation by controlling driving pressure for particle separation. Finally, the application of UV-curable glue moulds for rapid duplication and alignment of multilayer microfluidic sorting devices was presented as an interesting method for device fabrication. While we have shown proof of principle for a range of new methods, further optimization is required to fully benefit from these approaches.

Paper 1. Open DLD channel for particles and cell sorting

We show separation of biologically relevant particles, on patterned surfaces that are reusable, based on a variety of relevant parameters such as size and shape, without the need for external pumps. DLD has proven to be a powerful tool for bio-separations, and here we show proof of principle of an open DLD device that is easier to fabricate, reusable, simpler and therefore potentially cheaper, without using any external pumps. Our approach is relevant for applications in medicine, biological research, and forensics for sample preparation and purification. The potential low cost, ease of use and non-reliance on external equipment makes it particularly suitable for fieldwork, not least in challenging environments such as the developing world.

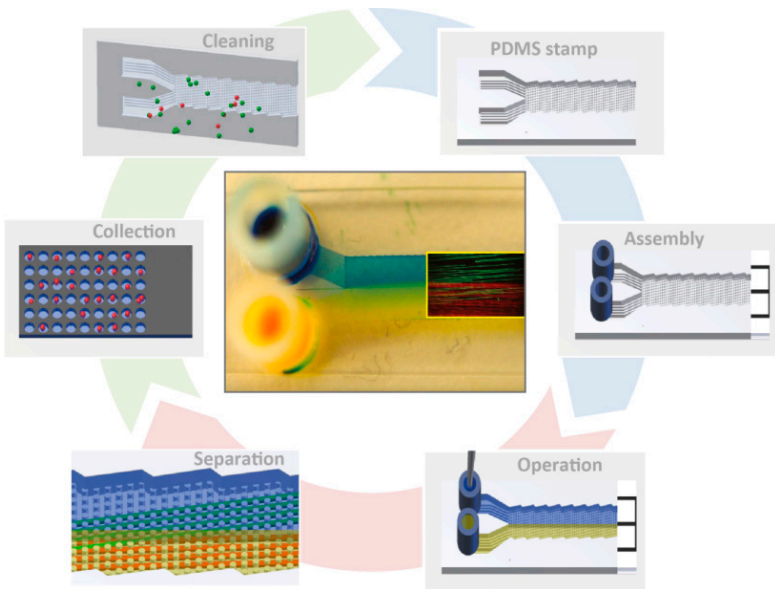

Figure 31. *Graphical abstract for the Open DLD approach: fabrication, operation, particle separation and collection to cleaning and reuse.*

Paper 2. Softness sorting for cancer cells in deterministic lateral displacement

Due to their direct association with the physiology of cells, physical properties are especially attractive as markers for sorting and characterization of cancer cells. Where molecular surface markers are lacking, the physical properties can instead serve as inherent markers for separation. This is especially interesting for cancer cells as softer cells are known to be more metastatic than hard cells. We have successfully demonstrated and measured the deformability of normal breast cells (MCF10A) and breast cancer cells (MCF7 and MDA-MB-231) using DLD devices. We find that the MDA-MB-231 cells are deformed more than 10% at the highest flow rates and that they are completely separated from the relatively much harder non-malignant cell type MCF10A. Proof of principle of sorting based on deformability has been shown between MDA-MB-231 and MCF7 cells and we will continue utilizing it for other cell types and further applications.

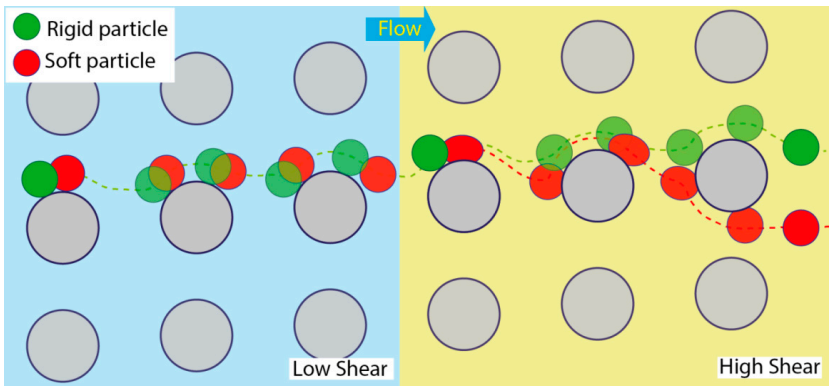

Figure 32. *Schematic of deformability-based sorting. While both rigid and soft particles displace at low pressure, the soft ones shift to zig-zag mode at higher pressure.*

Paper 3. Electrokinetic rotation of Red blood cells in DLD devices

Morphological separation in DLD relies on the controlled orientation of the particles of interest. Previous work has demonstrated orientation by confining the flow in the vertical direction. However, that may limit the achievable throughput. In this paper, instead of depth control, an alternative of applying a low frequency AC voltage (100 *Hz*) of a nominal value of 177 V_{RMS}/cm in a DLD device is demonstrated to control the orientation of the RBCs. By this method, the device will not be limited in depth, and we open up for higher throughput. An application of isolation of trypanosome parasite is the planned future work of this study.

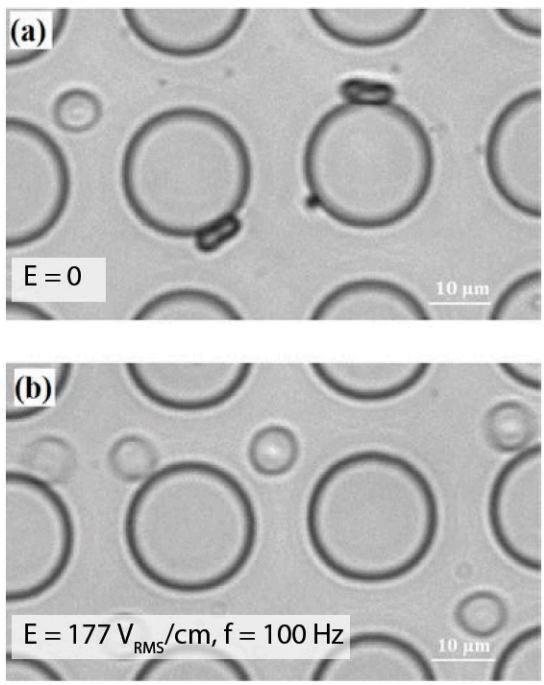

Figure 33. *Effect of electric field on orientation of RBCs in a DLD device. a) In the absence of an electric field, when the cells travell close to the pillars, they will lean against the pillars with their width, exhibiting a small effective size. b) RBC rotation due to the effect of an applied voltage.*

Paper 4. Rapid duplication and alignment for multilayers of microfluidic PDMS devices

In the soft-lithography process, PDMS stamps are duplicated many times from an SU8 master. This is associated with risks of damage to the master which in turn may cause waste of time and effort to redo the lithography process for the master. We have demonstrated a new method of duplicating a secondary master or mold using optical glue. The method has been developed to eliminate a punching step for fluidic access that is a standard step in conventional protocols of soft lithography. Furthermore, the capability of easily stacking multilayers of devices by alignment pins opens up for high throughput applications for PDMS devices.

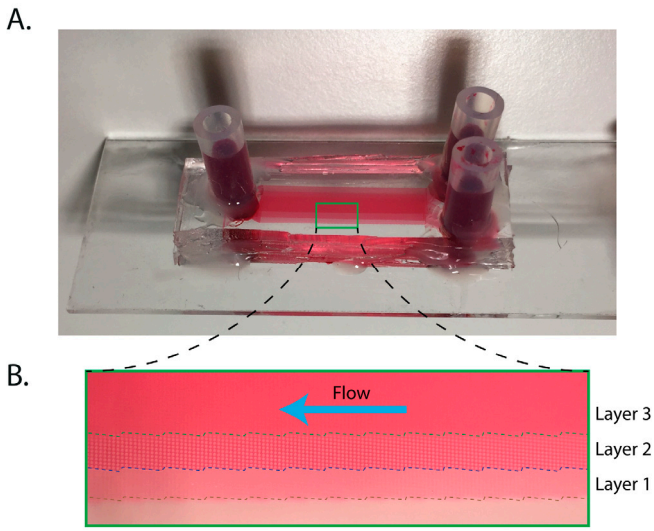

Figure 34. *Multilayers of a DLD device which are duplicated and aligned by a glue-based mold. A) An overview of the whole device. B) Food color helps to identify different layers of the device.*

Paper 5. Tunable separation in deterministic lateral displacement by pressure control on varying PDMS stiffness

In practice, many sorting experiments require careful optimization for obtaining high purity separations. As an attempt towards tunable particle separation in ongoing experiments, we carefully characterized the effects of deformation and the deformation of DLD devices by controlling the driving pressure. To avoid the effects of the elasticity of the PDMS, preparation was optimized with respect to mixing ratio, curing temperature and device thickness.

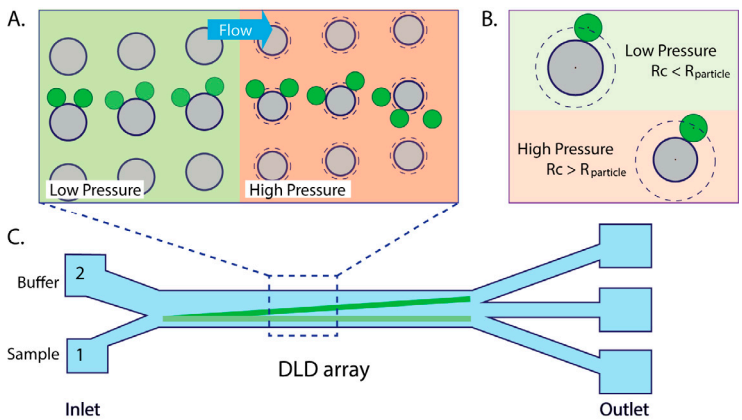

Figure 35. *Tunable separation in a DLD device. A) PDMS post deformation at high pressure. B) Particle trajectory tuned from displacement to zigzag mode. C) A sketch of the DLD device.*

Appendix

- DLD devices which were used mainly in Paper 2 & Paper 5 (multiple critical sizes). The device was designed by Stefan Holm.

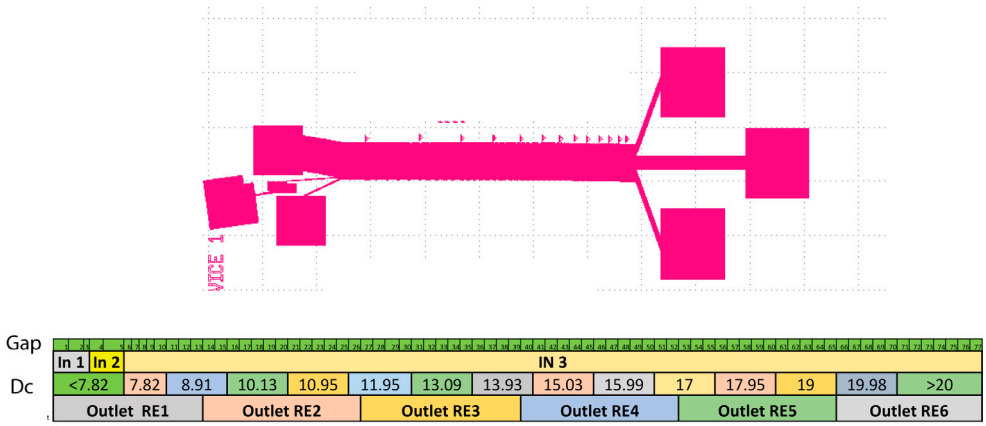

Figure 36. *DLD design and critical sizes.*

- DLD device which is used in Paper 1 (Single critical size).

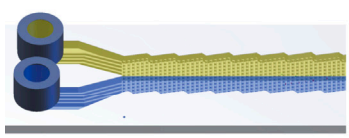

Open DLD device

Device	Dpost	Gap	Dc	Depth
1	30	11	5.1	24
2	30	23	10.7	24
3	30	31	14.4	24
4	20	12	5	24
5	20	12	5	9

Unit: µm

Figure 37*. Open DLD and all used devices.*

- Different built-in interfaces in Matlab programming were used to analyze the data.
    - –The scripts for size and shape measurement of cells (Fig. 38) as well as particle counting were developed by Thuy-Dung Nguyen.
    - –Extraction of specific features of cells of interest, which was used for single cell measurement has been created by Vuong D. Nguyen and associate prof. Ha T. Le (HMI Laboratory, Vietnam National University, Hanoi, Vietnam) (Fig.39).

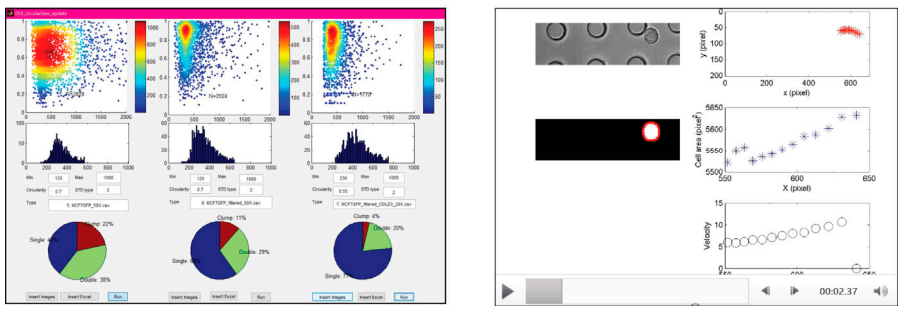

***Figure 38**. GUI for size and shape measument.*

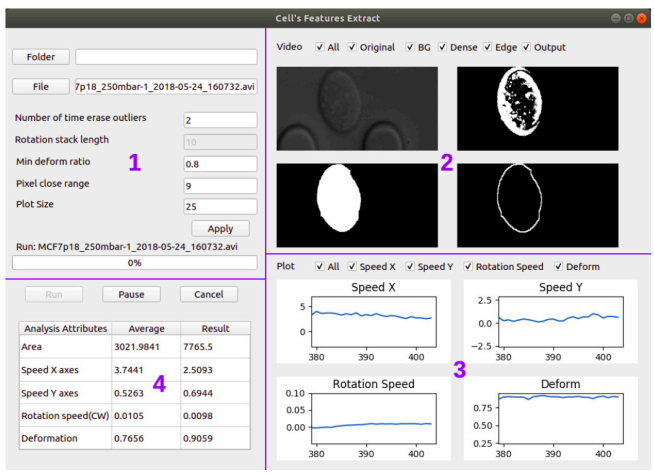

***Figure 39**. GUI for extraction of specific features of cells of interest.*

References

1. Pappas D (2016) Microfluidics and cancer analysis: cell separation, cell/tissue culture, cell mechanics, and integrated analysis systems. *Analyst* 141(2):525-535.
2. Halldorsson S, Lucumi E, Gomez-Sjoberg R, & Fleming RMT (2015) Advantages and challenges of microfluidic cell culture in polydimethylsiloxane devices. *Biosensors & bioelectronics* 63:218-231.
3. Tsai HF, Trubelja A, Shen AQ, & Bao G (2017) Tumour-on-a-chip: microfluidic models of tumour morphology, growth and microenvironment. *J R Soc Interface* 14(131).
4. Khan ZS & Vanapalli SA (2013) Probing the mechanical properties of brain cancer cells using a microfluidic cell squeezer device. *Biomicrofluidics* 7.
5. Kim YC, Park SJ, & Park JK (2008) Biomechanical analysis of cancerous and normal cells based on bulge generation in a microfluidic device. *Analyst* 133(10):1432-1439.
6. Otto O*, et al.* (2015) Real-time deformability cytometry: on-the-fly cell mechanical phenotyping. *Nature methods* 12(3):199-202, 194 p following 202.
7. Huh D, Gu W, Kamotani Y, Grotberg JB, & Takayama S (2005) Microfluidics for flow cytometric analysis of cells and particles. *Physiol Meas* 26(3):R73-98.
8. Haik Y, Pai V, & Chen CJ (1999) Development of magnetic device for cell separation. *Journal of magnetism and magnetic materials* 194:254-261.
9. Pappas D & Wang K (2007) Cellular separations: a review of new challenges in analytical chemistry. *Analytica chimica acta* 601(1):26-35.
10. Di Carlo D, Irimia D, Tompkins RG, & Toner M (2007) Continuous inertial focusing, ordering, and separation of particles in microchannels. *Proceedings of the National Academy of Sciences of the United States of America* 104(48):18892-18897.
11. Huang LR, Cox EC, Austin RH, & Sturm JC (2004) Continuous particle separation through deterministic lateral displacement. *Science* 304(5673):987-990.
12. Gossett DR*, et al.* (2010) Label-free cell separation and sorting in microfluidic systems. *Analytical and bioanalytical chemistry* 397(8):3249-3267.
13. Pamme N (2007) Continuous flow separations in microfluidic devices. *Lab on a chip* 7(12):1644-1659.

14. Yamada M, Nakashima M, & Seki M (2004) Pinched flow fractionation: Continuous size separation of particles utilizing a laminar flow profile in a pinched microchannel. *Analytical chemistry* (76):5465-5471.
15. Giddings JC (1966) A New Separation Concept Based on a Coupling of Concentration and Flow Nonuniformities. *Separation Science* 1(1):123-125.
16. Laurell T, Petersson F, & Nilsson A (2007) Chip integrated strategies for acoustic separation and manipulation of cells and particles. *Chemical Society reviews* 36(3):492-506.
17. Harrison DJ*, et al.* (1993) Micromachining a Miniaturized Capillary Electrophoresis-Based Chemical Analysis System on a Chip. *Science* 261(5123):895-897.
18. Pethig R, Menachery A, Pells S, & De Sousa P (2010) Dielectrophoresis: a review of applications for stem cell research. *J Biomed Biotechnol* 2010:182581.
19. Davis JA*, et al.* (2006) Deterministic hydrodynamics: taking blood apart. *Proceedings of the National Academy of Sciences of the United States of America* 103(40):14779-14784.
20. Holm SH, Beech JP, Barrett MP, & Tegenfeldt JO (2011) Separation of parasites from human blood using deterministic lateral displacement. *Lab on a chip* 11(7):1326-1332.
21. Tran TSH, Ho BD, Beech JP, & Tegenfeldt JO (2017) Open channel deterministic lateral displacement for particle and cell sorting. *Lab on a chip* 17(21):3592-3600.
22. Loutherback K, Puchalla J, Austin RH, & Sturm JC (2009) Deterministic microfluidic ratchet. *Phys Rev Lett* 102(4):045301.
23. Loutherback K*, et al.* (2010) Improved performance of deterministic lateral displacement arrays with triangular posts. *Microfluidics and Nanofluidics* 9(6):1143-1149.
24. Loutherback K*, et al.* (2012) Deterministic separation of cancer cells from blood at 10 mL/min. *AIP Adv* 2(4):42107.
25. Liu Z*, et al.* (2013) Rapid isolation of cancer cells using microfluidic deterministic lateral displacement structure. *Biomicrofluidics* 7(1):11801.
26. Zhang Z, Henry E, Gompper G, & Fedosov DA (2015) Behavior of rigid and deformable particles in deterministic lateral displacement devices with different post shapes. *The Journal of chemical physics* 143(24):243145.
27. D'Silva J, Austin RH, & Sturm JC (2015) Inhibition of clot formation in deterministic lateral displacement arrays for processing large volumes of blood for rare cell capture. *Lab on a chip* 15(10):2240-2247.
28. Liu Z*, et al.* (2015) Microfluidic cytometric analysis of cancer cell transportability and invasiveness. *Scientific reports* 5:14272.
29. Liu Z*, et al.* (2018) Integrated Microfluidic Chip for Efficient Isolation and Deformability Analysis of Circulating Tumor Cells. *Advanced Biosystems* 2(10):1800200.

30. Wei J, *et al.* (2015) Numerical Study of Pillar Shapes in Deterministic Lateral Displacement Microfluidic Arrays for Spherical Particle Separation. *IEEE Trans Nanobioscience* 14(6):660-667.
31. Zeming KK, Ranjan S, & Zhang Y (2013) Rotational separation of non-spherical bioparticles using I-shaped pillar arrays in a microfluidic device. *Nature communications* 4:1625.
32. Ranjan S, Zeming KK, Jureen R, Fisher D, & Zhang Y (2014) DLD pillar shape design for efficient separation of spherical and non-spherical bioparticles. *Lab on a chip* 14(21):4250-4262.
33. Au SH, *et al.* (2017) Microfluidic Isolation of Circulating Tumor Cell Clusters by Size and Asymmetry. *Scientific reports* 7(1):2433.
34. Karabacak NM, *et al.* (2014) Microfluidic, marker-free isolation of circulating tumor cells from blood samples. *Nat Protoc* 9(3):694-710.
35. Hyun J-c, Hyun J, Wang S, & Yang S (2017) Improved pillar shape for deterministic lateral displacement separation method to maintain separation efficiency over a long period of time. *Separation and Purification Technology* 172:258-267.
36. Inglis DW (2009) Efficient microfluidic particle separation arrays. *Applied Physics Letters* 94(0313510).
37. Vernekar R, Kruger T, Loutherback K, Morton K, & D WI (2017) Anisotropic permeability in deterministic lateral displacement arrays. *Lab on a chip* 17(19):3318-3330.
38. Kulrattanarak T, *et al.* (2011) Mixed motion in deterministic ratchets due to anisotropic permeability. *Journal of colloid and interface science* 354(1):7-14.
39. Kulrattanarak T, van der Sman RGM, Schroën CGPH, & Boom RM (2010) Analysis of mixed motion in deterministic ratchets via experiment and particle simulation. *Microfluidics and Nanofluidics* 10(4):843-853.
40. Kim SC, *et al.* (2017) Broken flow symmetry explains the dynamics of small particles in deterministic lateral displacement. *Proceedings of the National Academy of Sciences of the United States of America* 10(1074):5034-5041.
41. Holm SH, Beech JP, Barrett MP, & Tegenfeldt JO (2016) Simplifying microfluidic separation devices towards field-detection of blood parasites. *Anal. Methods* 8(16):3291-3300.
42. Campos-Gonzalez R, *et al.* (2018) Deterministic Lateral Displacement: The Next-Generation CAR T-Cell Processing? *SLAS Technol* 23(4):338-351.
43. Civin CI, *et al.* (2016) Automated leukocyte processing by microfluidic deterministic lateral displacement. *Cytometry. Part A : the journal of the International Society for Analytical Cytology* 89(12):1073-1083.
44. Wunsch BH, *et al.* (2019) Gel-on-a-chip: continuous, velocity-dependent DNA separation using nanoscale lateral displacement. *Lab on a chip* 19(9):1567-1578.

45. Wunsch BH*, et al.* (2016) Nanoscale lateral displacement arrays for the separation of exosomes and colloids down to 20 nm. *Nature nanotechnology* 11(11):936-940.
46. Laki AJ*, et al.* (2014) Microvesicle fractionation using deterministic lateral displacement effect. *Proceedings of the 9th IEEE International Conference on Nano/Micro Engineered and Molecular Systems*:490-493.
47. Laki AJ, Botzheim L, Iván K, Tamási V, & Civera P (2014) Separation of Microvesicles from Serological Samples Using Deterministic Lateral Displacement Effect. *BioNanoScience* 5(1):48-54.
48. Beech JP*, et al.* (2018) Separation of pathogenic bacteria by chain length. *Analytica chimica acta* 1000:223-231.
49. Zheng S, Yung R, Tai YC, & Kasdan H (2005) Deterministic lateral displacement MEMS device for continous blood separation. *18th IEEE International Conference on Micro Electro Mechanical Systems* (2005):851-854.
50. Zheng S, Tai YC, & Kasdan H (2005) A micro device for separation of Erythrocytes and Leukocytes in human blood. *Proceedings of the 2005 IEEE Enginering in medicine and biologi 27th annual conference* 1024-1027.
51. Inglis DW*, et al.* (2008) Determining blood cell size using microfluidic hydrodynamics. *Journal of immunological methods* 329(1-2):151-156.
52. Inglis DW, Lord M, & Nordon RE (2011) Scaling deterministic lateral displacement arrays for high throughput and dilution-free enrichment of leukocytes. *Journal of Micromechanics and Microengineering* 21(5):054024.
53. Holmes D*, et al.* (2014) Separation of blood cells with differing deformability using deterministic lateral displacement(dagger). *Interface focus* 4(6):20140011.
54. Kruger T, Holmes D, & Coveney P (2014) Deformability-based red blood cell separation in deterministic lateral displacement devices - A simulation study. *Biomicrofluidics* 8(054114-2).
55. Chen Y, Silva J, Austin RH, & Sturm JC (2015) Microfluidic chemical processing with on-chip washing by deterministic lateral displacement arrays with separator walls. *Biomicrofluidics* 9(054105).
56. Henry E*, et al.* (2016) Sorting cells by their dynamical properties. *Scientific reports* 6:34375.
57. Zeming KK, Salafi T, Chen CH, & Zhang Y (2016) Asymmetrical Deterministic Lateral Displacement Gaps for Dual Functions of Enhanced Separation and Throughput of Red Blood Cells. *Scientific reports* 6:22934.
58. Chou CY, Lu YT, Cahng CM, & Liu CH (2018) Selectively capturing monocytes from whole blood on microfluidic biochip for sepsis dianosis. *Proceedings of the 13th IEEE international conference on Nano/Micro Engineered and molecular systems*:56-59.
59. Zeng Y*, et al.* (2018) Microfluidic enrichment of plasma cells improves treatment of multiple myeloma. *Mol Oncol* 12(7):1004-1011.

60. Kabacaoğlu G & Biros G (2018) Sorting same-size red blood cells in deep deterministic lateral displacement devices. *Journal of Fluid Mechanics* 859:433-475.
61. Li N, Kamei DT, & Ho CM (2007) On-Chip continous blood cell subtype separation by determinisitic lateral displacement. *Proceedings of the 2nd IEEE International conference on Nano/Micro engineered and molecular system*:932-936.
62. Inglis DW*, et al.* (2008) Microfluidic device for label-free measurement of platelet activation. *Lab on a chip* 8(6):925-931.
63. Morton KJ*, et al.* (2008) Crossing microfluidic streamlines to lyse, label and wash cells. *Lab on a chip* 8(9):1448-1453.
64. Huang R*, et al.* (2008) A microfluidics approach for the isolation of nucleated red blood cells (NRBCs) from the peripheral blood of pregnant women. *Prenat Diagn* 28(10):892-899.
65. Green JV, Radisic M, & Murthy SK (2009) Deterministic Lateral Displacement as a Means to Enrich Large Cells for Tissue Engineering. *Anal. Chem* 81(21):9178-9182.
66. Zhang B, Green JV, Murthy SK, & Radisic M (2012) Label-free enrichment of functional cardiomyocytes using microfluidic deterministic lateral flow displacement. *PLoS One* 7(5):e37619.
67. Tottori N, Nisisako T, Park J, Yanagida Y, & Hatsuzawa T (2016) Separation of viable and nonviable mammalian cells using a deterministic lateral displcement microfluidic device. *Biomicrofluidics* 10(014125).
68. Joensson HN, Uhlen M, & Svahn HA (2011) Droplet size based separation by deterministic lateral displacement-separating droplets by cell--induced shrinking. *Lab on a chip* 11(7):1305-1310.
69. Tottori N, Hatsuzawa T, & Nisisako T (2017) Separation of main and satellite droplets in a deterministic lateral displacement microfluidic device. *RSC Advances* 7(56):35516-35524.
70. Inglis DW, Herman N, & Vesey G (2010) Highly accurate deterministic lateral displacement device and its application to purification of fungal spores. *Biomicrofluidics* 4(2).
71. Khodaee F, Movahed S, Fatouraee N, & Daneshmand F (2015) Numerical Simulation of Separation of Circulating Tumor Cells from Blood Stream in Deterministic Lateral Displacement (DLD) Microfluidic Channel. *Journal of Mechanics* 32(04):463-471.
72. Okano H*, et al.* (2015) Enrichment of circulating tumor cells in tumor-bearing mouse blood by a deterministic lateral displacement microfluidic device. *Biomedical microdevices* 17(3):9964.
73. Zhou J*, et al.* (2019) Isolation of circulating tumor cells in non-small-cell-lung-cancer patients using a multi-flow microfluidic channel. *Microsystems & Nanoengineering* 5(1).
74. Sarioglu AF*, et al.* (2015) A microfluidic device for label-free, physical capture of circulating tumor cell clusters. *Nature methods* 12(7):685-691.

75. Holm SH, J.P B, & Tegenfeldt JO (2013) Combined density and size-based sorting in deterministic lateral displacement devices *17th International conference on miniaturized systems for chemistry and life sciences*:1224-1226.
76. Beech JP & Tegenfeldt JO (2008) Tuneable separation in elastomeric microfluidics devices. *Lab on a chip* 8(5):657-659.
77. Beech JP, Jonsson P, & Tegenfeldt JO (2009) Tipping the balance of deterministic lateral displacement devices using dielectrophoresis. *Lab on a chip* 9(18):2698-2706.
78. Beech JP & Tegenfeldt JO (2009) Capillary driven separation on patterned surfaces. *Thirteenth International Conference on Miniaturized Systems for Chemistry and Life Sciences*:785-787.
79. Jiang M, Mazzeo AD, & Drazer G (2016) Centrifuge-based deterministic lateral displacement separation. *Microfluidics and Nanofluidics* 20(1).
80. Du S & Drazer G (2016) Gravity driven deterministic lateral displacement for suspended particles in a 3D obstacle array. *Scientific reports* 6:31428.
81. Hanasoge S, Devendra R, Diez FJ, & Drazer G (2014) Electrokinetically driven deterministic lateral displacement for particle separation in microfluidic devices. *Microfluidics and Nanofluidics* 18(5-6):1195-1200.
82. Hanahan D & Weinberg RA (2000) The hallmarks of cancer. *Cell* 100:57-70.
83. Guck J*, et al.* (2005) Optical deformability as an inherent cell marker for testing malignant transformation and metastatic competence. *Biophysical journal* 88(5):3689-3698.
84. Ribeiro AJ, Khanna P, Sukumar A, Dong C, & Dahl KN (2014) Nuclear stiffening inhibits migration of invasive melanoma cells. *Cell Mol Bioeng* 7(4):544-551.
85. Kuznetsova TG, Starodubtseva MN, Yegorenkov NI, Chizhik SA, & Zhdanov RI (2007) Atomic force microscopy probing of cell elasticity. *Micron* 38(8):824-833.
86. Li QS, Lee GY, Ong CN, & Lim CT (2008) AFM indentation study of breast cancer cells. *Biochem Biophys Res Commun* 374(4):609-613.
87. Dokukin ME, Guz NV, & Sokolov I (2013) Quantitative study of the elastic modulus of loosely attached cells in AFM indentation experiments. *Biophysical journal* 104(10):2123-2131.
88. Guz N, Dokukin M, Kalaparthi V, & Sokolov I (2014) If cell mechanics can be described by elastic modulus: study of different models and probes used in indentation experiments. *Biophysical journal* 107(3):564-575.
89. Musielak M (2009) Red blood cell-deformability measurement: review of techniques. *Clin Hemorheol Microcirc* 42(1):47-64.
90. McFaul SM, Lin BK, & Ma H (2012) Cell separation based on size and deformability using microfluidic funnel ratchets. *Lab on a chip* 12(13):2369-2376.
91. Dressaire E & Sauret A (2017) Clogging of microfluidic systems. *Soft matter* 13(1):37-48.

92. Wong I & Ho CM (2009) Surface molecular property modifications for poly(dimethylsiloxane) (PDMS) based microfluidic devices. *Microfluid Nanofluidics* 7(3):291-306.
93. Berthier J, Brakke KA, & Berthier E (2016) *Open Microfluidics* (Wiley).
94. Morton K*, et al.* (2010) The anti-lotus leaf effect in nanohydrodynamic bump arrays. *New Journal of Physics* 12(8):085008.
95. Fu E, Ramsey SA, Kauffman P, Lutz B, & Yager P (2011) Transport in two-dimensional paper networks. *Microfluid Nanofluidics* 10(1):29-35.
96. Osborn JL*, et al.* (2010) Microfluidics without pumps: reinventing the T-sensor and H-filter in paper networks. *Lab on a chip* 10(20):2659-2665.
97. Li X, Ballerini DR, & Shen W (2012) A perspective on paper-based microfluidics: Current status and future trends. *Biomicrofluidics* 6(1):11301-1130113.
98. Glavan AC*, et al.* (2013) Rapid fabrication of pressure-driven open-channel microfluidic devices in omniphobic R(F) paper. *Lab on a chip* 13(15):2922-2930.
99. Yang L, Hao X, Wang C, Zhang B, & Wang W (2013) Rapid and low cost replication of complex microfluidic structures with PDMS double casting technology. *Microsystem Technologies* 20(10-11):1933-1940.
100. Olmos CM*, et al.* (2019) Epoxy resin mold and PDMS microfluidic devices through photopolymer flexographic printing plate. *Sensors and Actuators B: Chemical* 288:742-748.
101. Girardo S*, et al.* (2018) Standardized microgel beads as elastic cell mechanical probes. *Journal of Materials Chemistry B* 6(39):6245-6261.

Printed by Media-Tryck, Lund 2019 NORDIC SWAN ECOLABEL 3041 0903

LUND UNIVERSITY

Lund University
Faculty of Engineering,
Department of Physics

ISBN 978-91-7895-139-0